Laser Remote Sensing and Technology

The Laboratory for Terrestrial Physics contains three organizations which are primarily laser remote sensing and technology oriented - the Geoscience Technology Office, the Space Geodesy and Sensor Calibration Office, and the Laser Remote Sensing Branch.

The **Geoscience Technology Office** develops advanced mission concepts and the associated components and instrumentation required to carry them out. It is composed of personnel with broad experience in the analysis and development of both active and passive optical sensors and often supports the activities of the other two technical organizations within the Laboratory. Under priorities established by Laboratory upper management, the GTO performs advanced mission analyses and simulations, evaluates and selects from among technical options for making a new or improved scientific measurement, identifies the technological "tall poles," develops the enabling hardware and software, performs appropriate field (ground, air, or space) experiments to demonstrate the technology, and works with other Laboratory entities to infuse these new technologies into future ground networks or spaceborne science missions.

The **Space Geodesy Networks and Sensor Calibration Office** manages and operates the NASA Satellite Laser Ranging (SLR) and Very Long Baseline Interferometry (VLBI) Networks in support of global space geodesy and Solid Earth geodynamics. The Office also provides the Earth science research community with a broad range of expertise in calibration and characterization of optical remote sensing instrumentation from the ultraviolet to the near infrared and through all phases of spaceflight.

The **Laser Remote Sensing Branch's** mission is to develop laser remote sensing techniques and instruments for scientific measurements of the Earth and planets. Activities include developing and demonstrating new measurement techniques, conducting experiments, and developing ground-based, airborne, and spaceborne laser sensors (lidars). The Branch's work is usually multidisciplinary, and involves theoretical and experimental activities in applied physics, technology development and instrument engineering. Some activities include planning and participating in scientific field campaigns, analyzing the laser measurement and laser sensor performance, acquiring and interpreting lidar data, and developing lasers, optics, and detector components. The Branch's work often involves collaborations with application scientists within Goddard, at universities or other government laboratories, and with researchers and engineers who specialize in lasers and electro-optics.

The accomplishments of these organizations have been broken down by topic: Spaceborne, Airborne, and Ground-based lidars, Laser Technology R&D, Satellite Laser Ranging, and Calibration.

Spaceborne Lidars

Geoscience Laser Altimeter System (GLAS) on the ICESat Mission

The Geoscience Laser Altimeter System (GLAS) is a new space lidar developed for long-term continuous measurements in Earth orbit [1]. Its design combines an altimeter with 5 cm precision with a laser pointing angle determination system and a dual wavelength cloud and aerosol lidar. GLAS was completed in June 2002, has been integrated with the ICESat spacecraft, and the integrated observatory was delivered to the Vandenberg launch site in the fall of 2002. The ICESat mission successfully launched January 12th, 2003 from a Boeing Delta II rocket into a 590 km altitude circular polar orbit. Photos of the launch are shown in Figure1. The ICESat mission parameters are summarized in Table1. GLAS was developed by NASA-Goddard and is

designed to operate continuously for 3-5 years. The ICESat spacecraft was developed by Ball Aerospace, and it and GLAS utilize data from GPS receivers developed by JPL to determine orbit altitude, position and time.

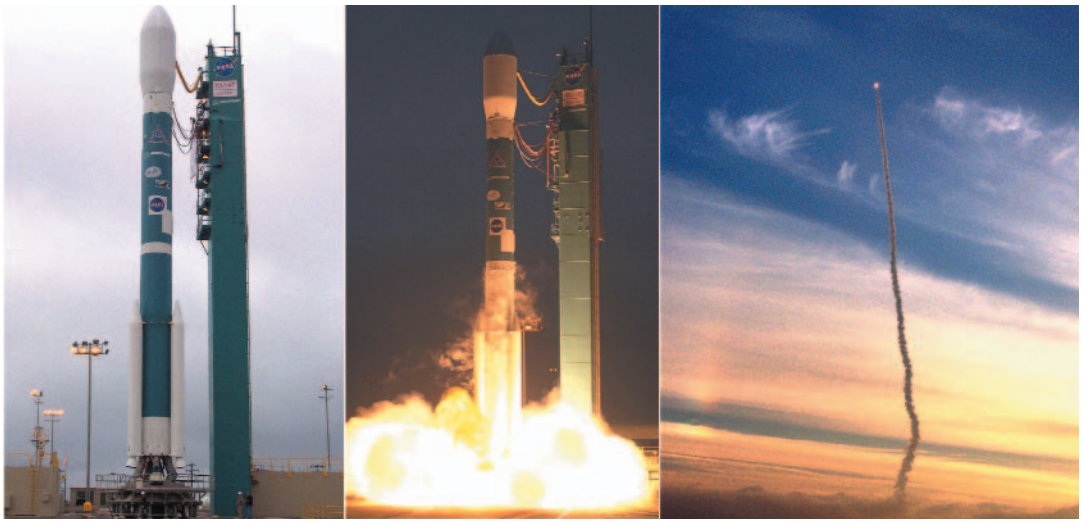

Figure 1. Photos of the launch of ICESat.

Table 1. ICESat Orbit & GLAS Measurements

Orbit altitude	598 km
Orbit inclination	94 degree
Orbit repeat tracks	Within 1 km every 183 days
Ground track spacing	15 km at equator 2.5 km at 80 deg latitude
Post-Processed pointing knowledge	≤ 2 arcsec (all axes)
Position requirements: Radial orbit height Along-track	Post-processing: < 5 cm < 20 cm
Laser measurement direction Off nadir pointing	Nadir viewing (nominal) < 5 degrees
Measurement wavelengths: Surface & cloud tops Atmospheric aerosols	 1064 nm 532 nm
Spot diameter on surface	66 m (e-2 points)
Along-track laser spot Separation	170 m

GLAS measures the range to the Earth's surface with 1064 nm laser pulses as illustrated in Figure 2. Each laser pulse produces a precision pointing measurement from the stellar reference system (SRS) and an echo pulse waveform, which permits range determination and waveform spreading analysis. The single shot ranging accuracy is < 10 cm for ice surfaces with slopes < 2 degrees. Changes in regional ice sheet heights will be determined by comparing successive GLAS measurement sets. GLAS will also measure atmospheric backscatter profiles at both 1064 and 532 nm [2]. The 1064 nm measurements use an analog Si-APD (Avalanche PhotoDiode) detector and measure the height, and profile the backscatter from thicker clouds. The measurements at 532 nm use photon counting detectors, and will measure the vertical height distributions of optically thin clouds and aerosol layers. A series of three ICESat missions are planned, which should dramatically improve our knowledge of the Earth's topography, atmosphere and ice sheets.

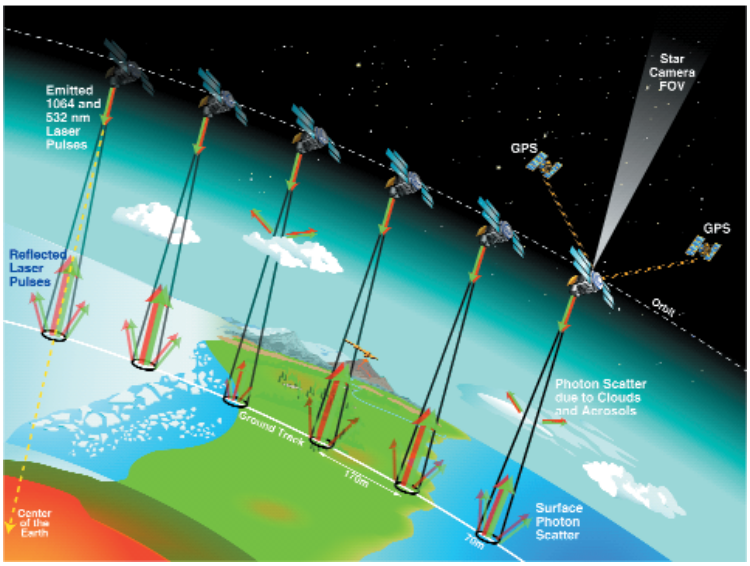

Figure 2: Schematic illustration of the GLAS instrument making measurements from ICESat while orbiting Earth. Graphic by Deborah McLean.

The completed GLAS instrument integrated to the spacecraft is shown in Figures 3a.-c. and its characteristics are summarized in Table 2. Subassemblies include three Q-switched ND:YAG lasers[3], an SRS which measures the pointing angles of each laser firing [4], a 100 cm diameter Beryllium receiver telescope, a 30 pm wide optical filter at 532 nm, and Si APD detectors for 1064 and 532 nm. The subassemblies are mounted on an L-shaped graphite epoxy optical bench. GLAS dissipates heat via 2 radiators, which are shown in Figure 3b and 4.

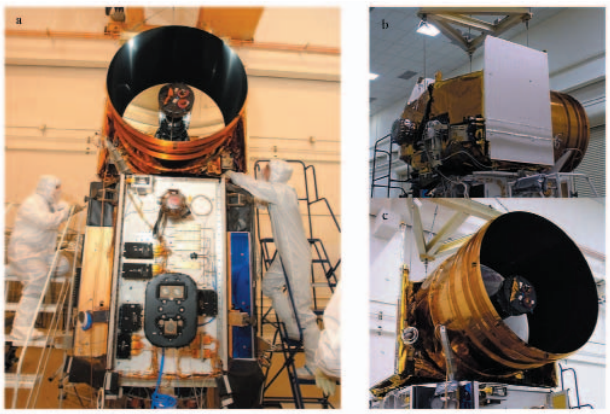

Figure 3. Photos of GLAS integration to spacecraft at Ball Aerospace, Boulder, Colorado. 3a. Shows Instrument mounted on top of spacecraft, 3b. GLAS wrapped with blanketing showing one of two radiators, 3c. View of GLAS 1-meter telescope.

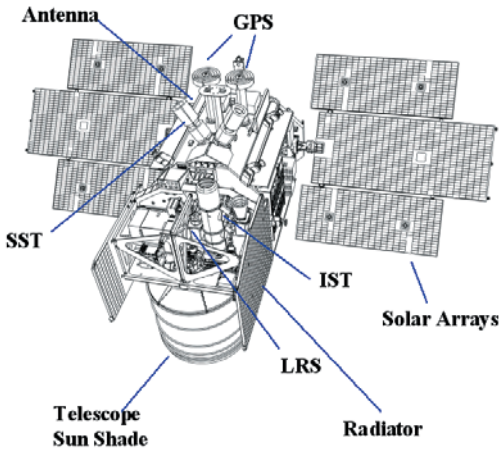

Zenith-Side View

Figure 4. Graphic of Zenith-Side View of ICESat satellite, GLAS plus spacecraft. IST- instrument star tracker, LRS - Laser Reference Sensor, SST- Spacecraft star tracker.

Table 2. GLAS Instrument Specifications

Laser Type	ND:YAG slab, 3 stage Passively Q-switched, Diode pumped
Number of lasers	3 each, one on at any time
Laser firing rate	40 pps
Laser pulse width	5 nsec
Laser Energy	75 mJ 1064 nm 32 mJ, 532 nm
Laser Divergence	110 urad; (exp(-2) pts)
Telescope diameter	100 cm
1064 nm detector	Si APD - analog (2 each)
532 nm detector	Si APD - Geiger (8 each)
Mass	330 kg
Power	300 W average
Instr. Duty cycle	100%
Data rate	~ 550 kbps (uncompress)
Physical size	~ 110 x 140 x 110 cm
Thermal control	Radiators with variable conductance heat pipes

The measurement performance of the completed GLAS instrument was evaluated using several new test instruments called the Bench Check Equipment (BCE). The main GLAS BCE was developed in parallel with GLAS and was used as an inverse altimeter and lidar. It was used to simulate the range of expected optical inputs to the GLAS receiver by illuminating its telescope with simulated background light and laser echoes with known powers and energy levels, widths and delay times. The BCE also allowed monitoring of the transmitted laser energy, the co-alignment of the transmitted laser beam to the receiver line of sight, and performance of the flight science algorithms. A separate BCE was developed to test the angle measurements of the SRS and profile of both the 1064 nm and 532 nm GLAS laser beams. These measurements were evaluated when GLAS was in air, before and after EMI and vibration tests, during and after the thermal vacuum chamber tests, and after delivery to the spacecraft. These measurements will also be used to compare pre-and post-launch performance of the instrument.

References

[1] H.J. Zwally, B. Schutz, W. Abdalati, J. Abshire, C. Bentley, A. Brenner, J. Bufton, J. Dezio, D. Hancock, D. Harding, T. Herring, B. Minster, K. Quinn, S. Palm, J. Spinhirne, R. Thomas, "ICESat's laser measurements of polar ice, atmosphere, ocean, and land," Journal of Geodynamics, Special Issue on Laser Altimetry 34, 405–445, 2002.

[2] J.D. Spinhirne, S.P. Palm, "Space based atmospheric measurements by GLAS" . In: Advances in Atmospheric Remote Sensing with Lidar, , A. Ansmann (Ed.), (Springer, Berlin, 1996) pp.213–217.

[3] R. S. Afzal, J. L. Dallas, A. Lukemire, W.A. Mamakos, A. Melak,, L. Ramos-Izquierdo, B. Schröder, A. W. Yu, " Space Qualification of the Geoscience Laser Altimeter System (GLAS) Laser Transmitters, In: Conference on Lasers and Electro-Optics, OSA Technical Digest, Optical Society of America, Washington, DC, 2002

[4] J.M. Sirota, P.S. Millar, E.A. Ketchum, B. E. Schutz and S. Bae, "System to attain accurate pointing knowledge of the Geoscience Laser Altimeter System, AAS 01-003, PP39-48, 2001.

Contact: James Abshire, James.B.Abshire@nasa.gov

Laser Pointing Angle Measurement for the Geoscience Laser Altimeter

The Geoscience Laser Atlimeter System, GLAS, for the Ice, Cloud, and Land Elevation Satellite (ICESat) mission, will make ice sheet elevation measurements in the polar regions to determine the mass balance of the ice sheets and their contribution to sea level change. In this high precision space based laser altimeter accurate knowledge of the laser beam's pointing angle is critical [1]. The GLAS design incorporates a stellar reference system (SRS) to relate the laser beam pointing angle to the star field to the required accuracy of 7.3 urad (1.5 arcsec). The SRS combines an attitude determination system (ADS) coupled to a 40 Hz laser reference system comprised of two narrow field of view cameras to perform this task.

The overall approach of the SRS is shown in Figure 5. The ADS measures the pointing of the instrument platform with respect to the star field while the laser reference sensor (LRS) samples the laser beam at 10 Hz and measures its alignment with respect to the components of the ADS. The Laser Profiling Array (LPA) measures the spatial profile of the laser beam at 40 Hz. The relative movement between the far field pattern of the GLAS laser beam, a reference source from the star tracker, and an occasional star will be determined. This data combined with the processed ADS data yields the pointing of the laser beam in inertial space.

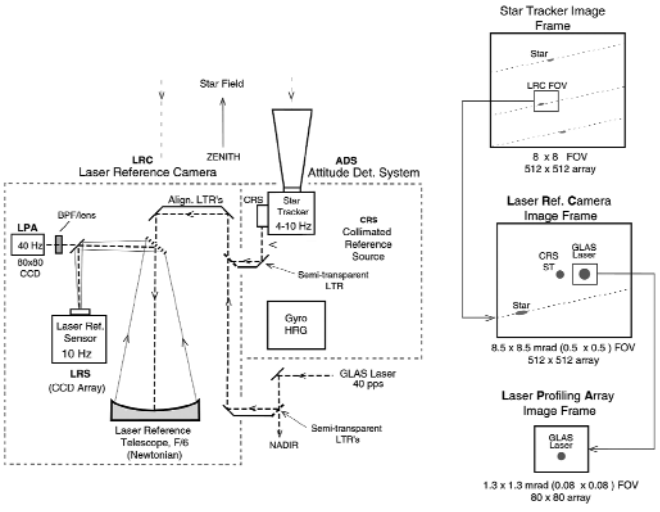

Figure 5. GLAS SRS Conceptual Approach. The GLAS laser beamis coupled into the LRS along with the CRS from the ADS. All optical beams are introduced concentrically through the semi-transparent diagonal mirror of the telescope.

The error budget allotment of the SRS is shown in Table 3. The ADS error component is dervied by combining the performance specifications from the gyro and star tracker with Kalman filtering [2]. Details of the laser reference system error component are listed in the table. This subsystem is the core instrument of the SRS, it combines the laser reference camera (CCD array plus telescope) with coupling optics and reference sources. All components of the LRS system have already been tested, with measured performance listed.

Table 3. SRS Error Budget

Laser Reference System Errors:	urad	arcsec	Comments	
Camera centroid resolution:	0.68	0.14	Laser image centroid	
	0.68	0.14	CRS image centroid	
	0.82	0.17	star image, 80 images through field	
Telescope distortion:	2.42	0.50	mirror deformation & figure uncertainty	
LTR's: internal alignment stability	1.94	0.40	couple to star camera	
	1.94	0.40	couple to glas laser	
	1.70	0.35	couple to glas laser	
ST boresight stability	2.42	0.50		
CRS-ST stability	1.45	0.30		
total LRS RSS error	5.38	1.05	1 sigma	
ADS Errors:	Roll		Pitch	
HD-1003 & HRG SIRU	urad	arcsec	urad	arcsec
1. Attitude Determination	1.45	0.30	1.45	0.30
2. Velocity Aberration	0.16	0.03	0.16	0.03
3. Star Position Accuracy	0.16	0.03	0.15	0.03
4. Ephemeris	0.03	0.01	0.03	0.01
ADS for each axis, (=RSS(2,3,4) +1)	1.68	0.35	1.67	0.35
ADS error (=RSS(roll & pitch))	2.37	0.49	1 sigma	
TOTAL SRS RSS ERRORS	5.61	1.16	1 sigma	

The SRS Bench Check Out Equipment (BCE), shown in Figure 6, was used to calibrate and verify the SRS instrument performance after integration to the main GLAS instrument. The overall thermal performance of the system was then verified during instrument thermal vacuum testing. The BCE incorporates a star field generator and a "ground truth" reference camera. Stars are generated with an array of 16 x 16 pinholes in a chromium coated silica plate. Light is sent to these pinholes by an array of multimode fibers. The light from the star generator is fed directly into the LRS. A large LTR is used to send a sample of the star field to the star tracker and to relay it to a ground reference camera (GRC). The flight laser is simultaneously imaged onto this GRC, which is considered "truth" during performance tests. The camera is capable of recording full images at 40 Hz, thus multiple stars plus the laser can be recorded. The BCE system was kept at constant temperature during performance verification tests, while the instrument was exposed to the full operational temperature range expected in flight. Performance in thermal-vacuum environment was assessed by comparing the infor-

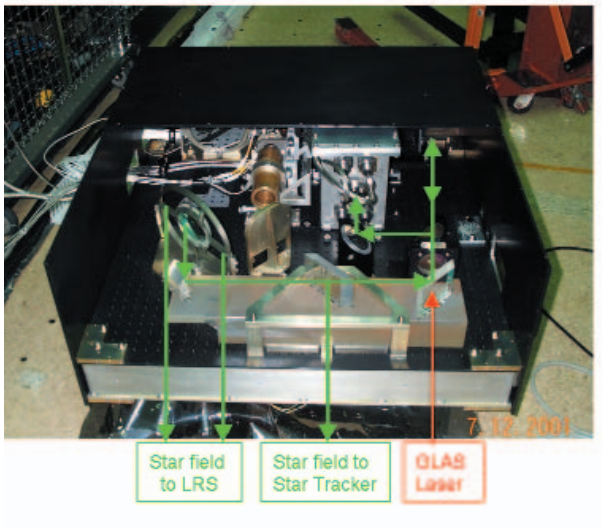

Figure 6. Photo of SRS BCE which stimulates the SRS with a star field and simultaneously measures the GLAS laser and star field with a ground Truth camera.

mation collected in the GRC to that collected by the flight instrument. During instrument thermal vacuum testing, the SRS complied with stability and performance requirements with margin. During spacecraft and instrument commissioning, 29 days after launch, the LRS successfully imaged the GLAS laser beam, the Collimated Reference Source (CRS) and dim stars every fifty seconds. The LRS sensitivity appears to be a factor of five more sensitive than required.

References:

1. Bufton, J.L., Garvin, J.B., Cavanaugh, J.F., Ramos-Izquierdo, L., Clem, T.D. and Krabill, W.B., "Airborne lidar for profiling of surface topography," Opt. Engr., 30:72 (1991).

2. S. Bae and B.E. Schutz, "Laser Pointing Determination Using Stellar Reference system in Geoscience Laser Altimeter System", AAS (00-123) 2000.

Contact: Pamela S. Millar, Pamela.S.Millar@nasa.gov

GLAS Main Bench Checkout Equipment

Testing and calibrating GLAS, and similar lidar systems, is a challenge partly due to the complexity of the expected ground surface echoes and cloud returns, and the stringent test environment. Testing of space instruments takes place in demanding environments such as clean rooms and thermal-vacuum chambers used to simulate on-orbit conditions.

The main Bench Checkout Equipment (BCE) was used to validate the science and engineering specifications of GLAS. This BCE was used to simulate the expected returns for GLAS at 1064 nm and 532 nm and also monitor important instrument parameters such as the laser power, oscillator stability and boresight alignment.

A functional block diagram of the Bench Checkout Equipment (BCE) is shown in Figure 7. It consists of several subsystems: The Altimeter Test System (ATS), the Lidar Test System (LdrTS), the Laser Test System (LsrTS), and the GPS/Timing System. A BCE controller acts as the central data conduit for the BCE subsystems. Two optical targets, a Main and Mini Target are used to optically couple signals into GLAS, perform laser diagnostics and test the boresight alignment of the instrument. The ATS was used to simulate and monitor ground and cloud returns and background at 1064 nm. The LdrTS was used to simulate and monitor ground and aerosol returns and background at 532 nm. The LsrTS was used to perform laser diagnostics. The Timing/GPS System was used to monitor the GLAS oscillator stability and provide a GPS signal to GLAS

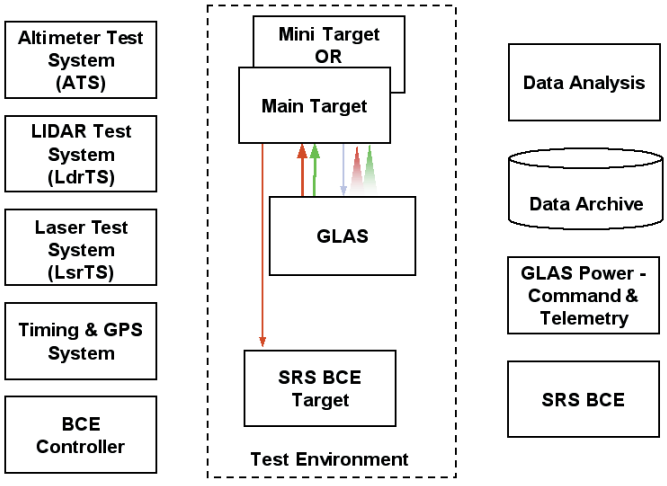

Figure 7. Functional Block Diagram of GLAS Bench Checkout Equipment

and the BCE subsystems. The two optical targets (Main and Mini) were used to retroreflect an attenuated laser beam back into the receiver, sweep the Field of View (FOV) of the 1064 nm detectors using a pair of motorized Risley prisms, and perform laser diagnostics. Additional subsystems were used to provide power, control and telemetry, data archiving, and science data analysis. A separate SRS optical target and BCE were also used to test the performance of the instrument stellar reference system as discussed in the previous section.

Contact: Haris Riris, Haris.Riris.1@gsfc.nasa.gov

Mercury Laser Altimeter (MLA)

The Mercury Laser Altimeter (MLA) is one of the primary instruments on NASA's MErcury Surface, Space ENvironment, GEochemistry and Ranging (MESSENGER) Project, part of the Discovery Program. MESSENGER, the first spacecraft ever to orbit the planet Mercury, will be launched in March 2004 and will enter Mercury orbit in April 2009, after two flybys of Venus and two of Mercury along the way. The flyby and orbital phases of the mission will provide global mapping and detailed characterization of the planet's surface, interior, atmosphere, and magnetosphere.

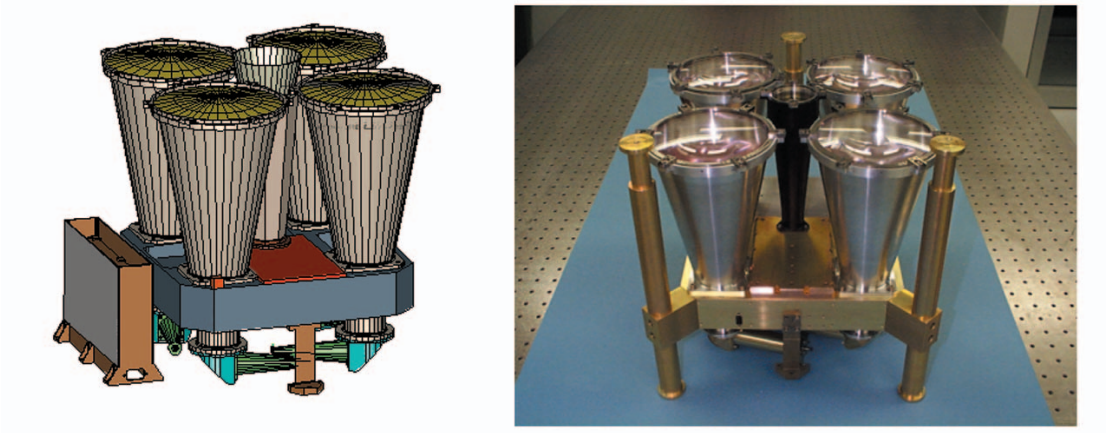

Figure 8: In 2002 MLA has moved from concept to reality. The CDR (critical design review) design is shown at left, and the engineering model is shown at right.

The MLA instrument, shown in Figure 8, is being designed and built as a PI mode instrument by a GSFC instrument team led by the Laser Remote Sensing Branch. The laser, shown in Figure 9, is being designed and built by laser remote sensing branch's Space Lidar Technology Center (SLTC) in College Park, MD, in collaboration with the engineering directorate.

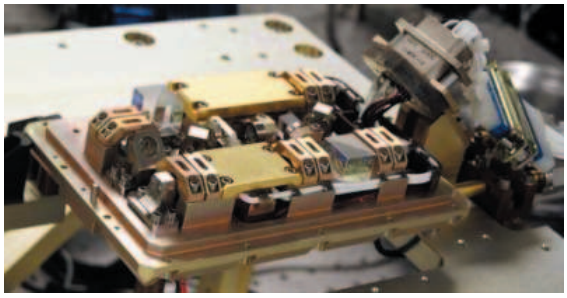

Figure 9: MLA Engineering Model laser has met or exceeded all performance requirements.

In 2002 MLA progressed from concept to reality. In February 2002, MLA successfully completed Critical Design Review (CDR) and was approved for implementation. The remainder of 2002 was spent in fabrication and assembly of engineering models and flight hardware subsystems. As of December 31, 2002, all subsystems have showed performance meeting or exceeding requirements, and the final as-delivered MLA Instrument is expected to show exceptional performance.

MLA was designed primarily to measure the libration, topography, and surface composition of Mercury. The MLA Instrument design leverages heavily from earlier successful developments from the Mars Orbiter Laser Altimeter (MOLA) and GLAS. Like MOLA, the receiver detection threshold is dynamically adjusted real-time via on-board software algorithms to be as low as possible while maintaining a predetermined false alarm rate, which is monitored via a noise counter whose output is fed back to the threshold control loop algorithm.

The MLA structure is constructed entirely of beryllium, with beryllium receiver tubes, laser bench and beam expander, and mounted to the MESSENGER spacecraft deck via three titanium flexures. The power converter assembly is housed in a magnesium chassis that mounts directly to the spacecraft deck.

The optical bandwidth of the MLA receiver, consisting of four transmitting receiver tube assemblies which fibercouple to the SiAPD detector, is 0.8 nm wide FWHM (full-width half maximum) and centered at 1064 nm. The receiver field of view is 400 μrad FWHM.

The laser is a Cr doped Nd:YAG design employing passive Q-switching. The expected output energy is 20 mJ, with an 8 Hz repetition rate and 5 nsec pulse width. Divergence is expected to be less than 50 μrad.

The timing and signal processing employs a unique design based around an APL-supplied "Time-of-Flight" ASIC which will allow superb time resolution, down to 400 ps. MLA has three matched filter pulse capture channels (10, 60, 270 nsec), and will allow detection of return pulse widths from 7-1000 nsec, with up to 15 returns captured per shot.

MLA looks forward to a successful delivery to the MESSENGER Spacecraft in May 2003.

Contact: Xiaoli Sun, Xiaoli.Sun-1@nasa.gov

The Mars Orbiter Laser Altimeter (MOLA) - Radiometry

The Mars Orbiter Laser Altimeter (MOLA) continued operation in its passive radiometry mode, producing near infrared images of Mars. MOLA has now recorded two years of seasonal radiometric changes. The calibration of the receiver responsivity was further refined to account for the unusually cold detector temperature after the external heater was powered off to conserve spacecraft power.

Figure 10 shows a series of MOLA false-color albedo images of Mars polar caps. Colors correspond to ratios of detected (incident) to radiant flux in the range 0-40%. Martian seasons are denoted by the longitude of Sun (Ls): 0° at the start of northern Spring, or equinox, and 180° at the southern equinox. The southern cap (left column) recedes from the start of spring (Ls=180°) to mid-summer (Ls=300°), with a dark interior region thought to represent slab CO_2 ice. The northern polar cap (right column) leaves bright outliers as it contracts. The interval between images is 30° of Ls, or roughly 57 Martian sols. Over the course of a year, roughly 30% of the atmosphere is exchanged between the poles as CO_2 frost accumulates and sublimates.

The investigation into the apparent failure of the clock oscillator was concluded. Extensive tests

were performed on a flight spare unit and a similar failure mode was partially reproduced. Gradual losses in the quartz crystal, and gain reduction due to accumulated space radiation damage to transistors, caused the signal amplitude of the oscillator circuit to vanish or become too low to trigger the CMOS buffer gate.

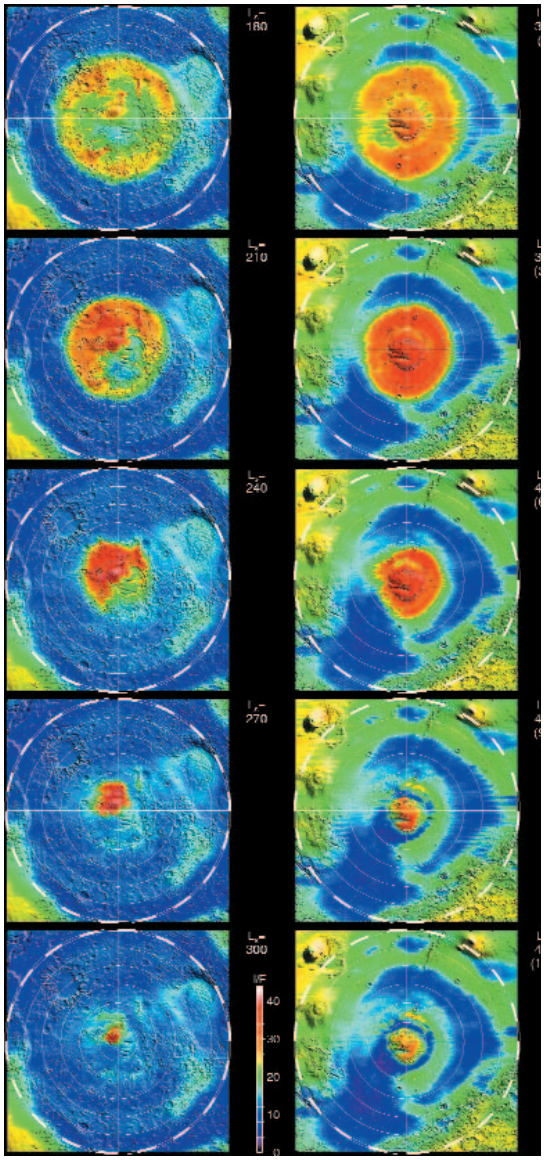

Figure 10. MOLA false-color albedo images of Mars polar caps.

Contact: Dr. Xiaoli Sun, Xiaoli.Sun-1@nasa.gov

Airborne and Ground Based Lidars

Laser Vegetation Imaging Sensor (LVIS) - Airborne Imaging Laser Altimetry

The Laser Vegetation Imaging Sensor (LVIS) is a wide-swath (2 km), full return-waveform, imaging, airborne laser altimeter developed at GSFC for measuring topography (including sub-canopy) and vegetation height and vertical structure. LVIS data has produced some of the best estimates of above-ground biomass in densely forested regions. LVIS has been selected as a part of the LBA project to map ~15,000 km^2 of topography and vegetation structure parameters in the Brazilian Amazon in 2003. The LVIS instrument has recently been redesigned to improve performance and to drastically reduce size, weight and power consumption. The updated instrument has been assembled and tested in the NOAA Cessna Citation jet aircraft. The upgraded LVIS system significantly expands the instrument's capabilities allowing the collection of full return-waveform imaging data at rep-rates exceeding 10 kHz. In addition to the Brazilian flight mission, the LVIS instrument has been selected to map ~3,000 km^2 of topography and vegetation structure parameters at 5 m horizontal resolution in the state of Maryland. Further improvements to the LVIS receiver and scanning systems are planned to increase the swath width to 4 km by the end of 2003.

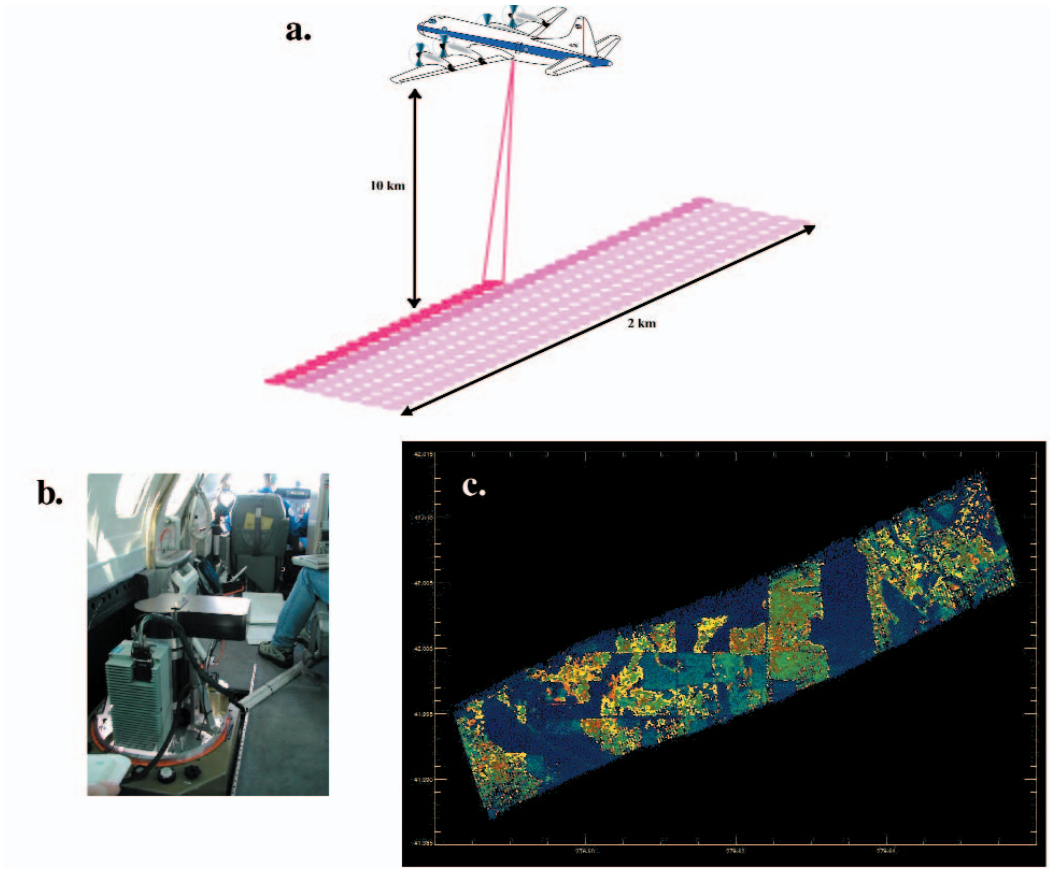

Figure 11. The top graphic (a) illustrates the scan pattern used by LVIS to produce images of topography and vegetation structure from an aircraft. The image on the bottom left (b) shows the compact new LVIS instrument seated in a standard air-photo camera mount in the NOAA Cessna Citation. The graphic on the bottom right (c) is an example swath of vegetation height data from the LVIS instrument.

Contact: Bryan Blair, James.B.Blair@nasa.gov

Airborne Multikilohertz Microlaser Altimeter (Microaltimeter)

The Microaltimeter, developed under NASA's Instrument Incubator Program (IIP), operates at multi-kHz rates from aircraft cruise altitudes with a single pulse energy of a few microJoules (mJ) and a 14 cm diameter off-axis telescope, which is spatially shared by the transmitter and receiver. The final configuration of the system uses a multi-anode metal channel dynode photomultiplier in order to segment the ground image into 16 elements (4x4 pixels). Each of the anodes is input to an independent timing channel so that the altimeter can be operated in a 3D imaging mode. For increased portability between aircraft, the instrument is packaged to fit into a standard Lyca camera mount, which is widely used in airborne experiments.

In September 2002 the final flight experiments were completed over Ocean City, Maryland and Assateague Island, Virginia regions, collecting over 3.3 Gigabytes of data, which represents over 1.5 hours of actual laser ranging to the surface, using a 4 mJ per pulse laser operating at 532 nm. The instrument was flown onboard the Wallops P3B aircraft from an altitude of 3300 m, using a circular scanning wedge to create a ground swath of about 120 m in diameter. With the laser fire rate of 8 kHz, and a scan rate of 10 Hz, the distance between laser footprints was around 50 cm. The flight took place in clear sky conditions during the early afternoon of September 12th, 2002.

The IIP Final Report for the Microaltimeter was delivered in November 2002, containing twelve papers written on various aspects of the project and an Executive Summary. While the IIP part of the Microaltimeter project has now ended, work continues in house on the analysis and validation of the flight data against an existing Digital Elevation Model (DEM) of the region, and EarthData Technologies, LLC will be working with the Microaltimeter ranging data through a Memorandum of Agreement with NASA. As a spin-off to the technology, the next Shuttle Laser Altimeter experiment (SLA03) will make use of the concepts and hardware design of the Microaltimeter.

The following figure shows the work in progress on the post processing. The results are from the May 2001 Microaltimeter flight over buildings in Ocean City from an altitude of 1650 m with the scanner rotating at 10 Hz. The ground swath is roughly 15 m in diameter by 120 m in length, with a vertical dimension of 10 m. The point cloud plot on the left gives the terrain heights from the ground (blue) and the buildings (green, yellow and orange) after post processing of ranging information. The plot on the right is a bar plot of the same data, filling in the gaps between the points by interpolation.

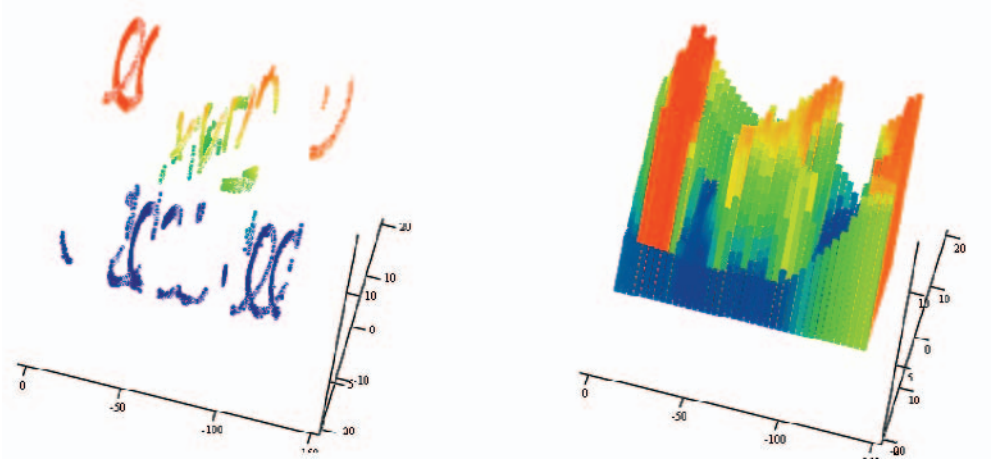

Figure 12. 3D terrain heights of Ocean City buildings from May 2001 Microaltimeter flight ranges. The left plot is a point cloud plot and the right plot is the same data shown as an interpolated bar plot.

Contact: Jan McGarry, Jan.F.McGarry@nasa.gov

Spectral Ratio Biospheric Lidar

The Normalized Difference Vegetation Index (NDVI) and related vegetation indices (VI) rely on the distinctive optical properties (reflectivity and absorption) of chlorophyll containing vegetation. The dominant pigment in plant leaves, Chl a, strongly absorbs visible light (from 0.4 to 0.7 μm) for use in photosynthesis, with blue and red peaks near 0.43 and 0.67 μm. However, the cell structure of the leaves strongly reflects near-infrared light (from 0.7 to 1.2 μm). This transition around 0.7 μm is referred to as the red edge. In general, if there is much less reflected radiation in red wavelengths than in near-infrared wavelengths, then the vegetation is likely healthy and dense whereas if there is little difference in the intensity of the reflected red and near-infrared wavelengths then plant leaves are likely sparse, absent, or dead.

A land-surface lidar that uses spectral reflectance to discriminate living vegetation from non-living sources of surface roughness would have great potential for airborne mapping and for future NASA missions. In particular, Earth-orbiting lidar missions to map biomass carbon and to measure dynamic topography and ecosystem change could yield much more accurate and specific data, if they include vertically-resolved discrimination of the types of surfaces measured. A lidar instrument that actively measures vegetation spectral response, in two narrow wavelength bands on either side of the red edge would also provide unprecedented information for calibration of passively acquired multi-spectral vegetation data (e.g. AVHRR). This is due to the precise pointing capability, narrow laser divergence (i.e., small spot size on the surface) and narrow fields of view possible with lidar instruments. Also, by keeping the two probe wavelengths close to the red edge, the lidar can measure and remove along-path reflectance from atmospheric aerosols. Therefore, any differences in measured spectral reflectance at the two probe wavelengths are due to differences in the surface features and not the atmospheric path. Precursor techniques used fundamental (1064 nm) and doubled (532 nm) Nd:YAG lidar signals or ratios of active near-IR reflectance signals for target discrimination and ranging. Paired wavelengths near the vegetation red edge have not been used in existing lidar systems.

A laboratory demonstration instrument was developed this year, using low power diode lasers operating at 670 and 775 nm. This instrument will be used to show that the underlying measurement concept is feasible. However, the 50-70 mW output power of these lasers is not sufficient to demonstrate the concept from an aircraft or from orbit. And there are currently no space-qualified, high power lasers available at these wavelengths, 670 nm and 775 nm. The most attractive path for scaling transmitter power to that needed for high-altitude airborne platforms and on-orbit applications appears to be frequency doubling the output of rare-earth-doped fiber amplifiers and Raman amplifiers developed for the telecommunications industry (1.2-1.6 μm). These devices and related components have been built for demanding applications, e.g., undersea fiber-optic links, with established reliability.

For FY03 a prototype spectral-ratio biospheric lidar system will be built using robust, commercial-off-the-shelf (COTS) telecommunication components (e.g Er/Yb doped fiber amplifiers, Raman amplifiers) in conjunction with TRL-4 (Technology Readiness Level 4) non-linear optical components for frequency doubling (e.g. periodically poled KTP) generating several watts of laser power at 670 and 775 nm. Active measurements will be demonstrated of vegetation spectral responses, at power levels appropriate for resolving surface types within shadowed canopy volumes and suitable for high-altitude airborne use or possibly, on-orbit systems.

A breakthrough in this area, and work to define a pathway to space, could provide the Laboratory and Goddard with a crucial advantage in competing for future NASA Earth Science missions. The Jet Propulsion Laboratory (JPL) flew a 1550 nm fiber laser as part of the Shuttle Radar Topography mission (SRTM), and work is on-going at several institutions to develop space-based fiber laser communication systems for data down-link. Other R&D funding at GSFC has supported work to adapt telecommunications components for use in space laser transmitters. Related work is developing sub-

systems for column CO_2 measurements (CO_2 Laser Sounder) using some of the same components identified for this proposal (e.g. Distributed Feed Back or DFB laser diodes operating at 1572 nm).

See annual report topic "Fiber Amplifier Power Scaling/Frequency Doubling" J. Rall, this report.

Contact: Jonathan A. R. Rall, Jonathan.A.Rall@nasa.gov

Automatic Weather Station (AWS) Lidar

A ground based, autonomous, low-power atmospheric lidar instrument is being developed at NASA Goddard Space Flight Center. This compact, portable lidar will operate continuously in an insulated enclosure, charge its own batteries through a combination of a small rugged wind generator and solar panels, and transmit its data from remote locations to ground stations via satellite. The goal is to co-locate these instruments at several of the many remote Automatic Weather Station (AWS) sites in Antarctica. The NSF Office of Polar Programs provides support to place weather stations in remote areas of Antarctica in support of meteorological research and operations around the continent. The AWS meteorological data will directly benefit the analysis of lidar data while a network of ground based atmospheric lidar will provide knowledge regarding the temporal evolution and spatial extent of Type Ia polar stratospheric clouds (PSC). These clouds play a crucial role in the annual austral springtime destruction of stratospheric ozone over Antarctica, i.e. the ozone hole. In addition, the lidar will monitor and record the general atmospheric conditions (transmission and backscatter) of the overlying atmosphere which will benefit the Geoscience Laser Altimeter System (GLAS) aboard the recently launched ICESat mission. A conceptual design of the Automatic Weather Station Lidar is shown in Figure 13. A prototype lidar was developed and deployed to the Automated Geophysical Observatory (AGO) P1 in January 1999. AGO Lidar was designed to operate inside the heated AGO enclosure and to consume less than 15 W of power continuously.

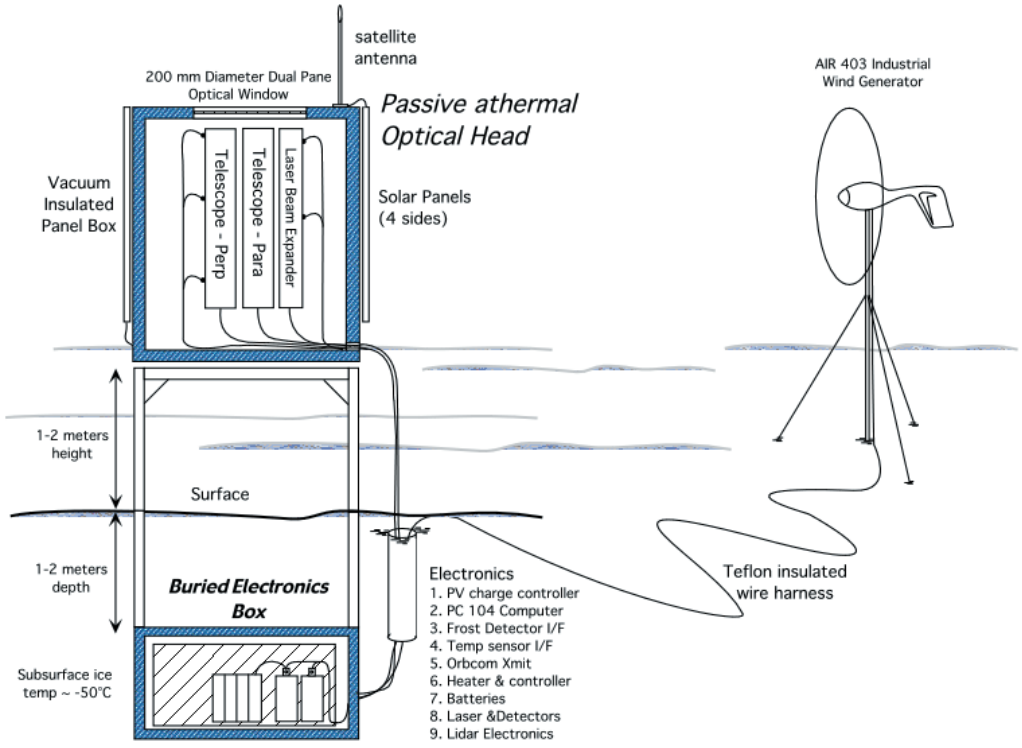

Figure 13. Conceptual design of the Automatic Weather Station Lidar.

Lessons learned from AGO Lidar have influenced the design of the AWS Lidar instrument. A completely autonomous, free-standing approach was adopted. In order to minimize electrical generation and heating requirements, a two-enclosure approach was chosen which simplified the thermal design and thermal management of the instrument. One temperature controlled box containing all of the power dissipating electronics and electro-optics will be buried approximately 1 m below the surface while the other box (not temperature controlled) will be mounted on poles about 1 meter above the surface. This above surface box will contain the fiber-optic coupled, athermal refractive telescopes and the out-going laser beam expander.

The working design of the instrument employs a frequency-doubled, diode-pumped, Nd:YAG microchip laser which is fiber coupled to the outgoing beam expander. However, concurrent work developing high-power, frequency-doubled fiber amplifiers may supersede this approach. (See Annual Report 2002 topic: Fiber Amplifier Power Scaling/Frequency Doubling.) The fiber coupled beam expander used to transmit the outgoing laser energy and the two receiver telescopes, used to sense depolarization of the scattered light, will employ a novel athermal telescope which was designed, built and tested at Goddard Space Flight Center. This fiber-coupled telescope, shown in Figure 14 undergoing temperature testing in an environmental chamber, maintained focus and alignment from –50°C to +30°C, an 80°C temperature range. To increase the effective aperture of the receiver, multiple telescopes can be added.

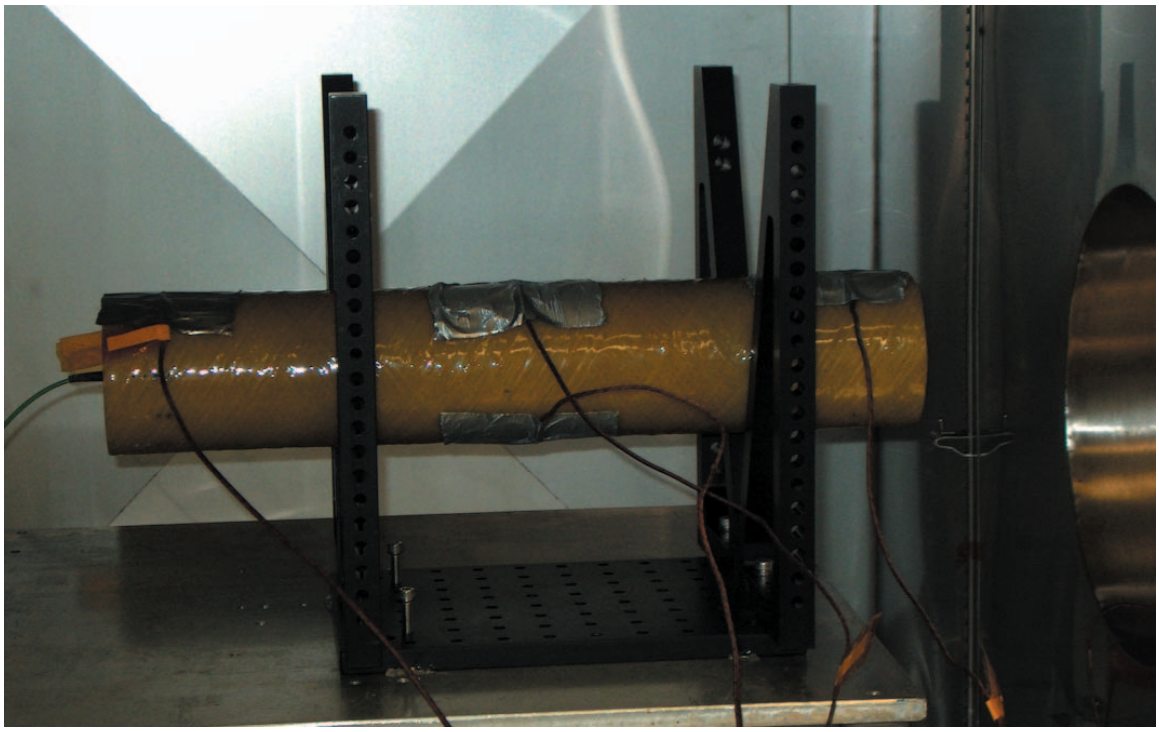

Figure 14. Athermal refractive telescope

To power the lidar instrument and satellite transceiver, storage batteries contained in the sub surface enclosure will be charged by a combination of four 30 W solar arrays and a rugged, 400 W wind generator (Figure 15). The four, 30 Watt solar panels will be mounted on each side of the above surface enclosure to take advantage of the continuous low-elevation solar angle during the austral summer. The small, rugged wind generator will be installed on a guy-stabilized, 3-4 m pole nearby to charge the batteries during the six-month, polar night.

Figure 15. Marine wind generator and solar panels undergoing testing at NASA Goddard Space Flight Center.

The buried box approach takes advantage of the nearly constant subsurface ice temperature of -50°C which greatly simplifies thermal design of the instrument and the excellent insulating properties of the surrounding snow and ice. This box will be heated by a combination of waste heat from the electronics and electro-optics (~10 watts) and an additional heating element to maintain an acceptable operating temperature range. The above surface box will be mounted on four poles augered into the ice. This is to take advantage of the wind-scouring effect that tends to keep smooth, elevated flat surfaces free of ice and snow accumulation and to reduce or eliminate snow drifting/accumulating around the base.

Incremental deployment of AWS Lidar hardware is set to begin during the 2003-2004 summer servicing season.

References:

[1] J. A. R. Rall, J. Cavanaugh, J. Campbell James B. Abshire & James D. Spinhirne, "Automated Geophysical Observatory (AGO) Lidar," Abstract accepted for presenatation at the 2002 International Geoscience And Remote Sensing Symposium (IGARSS), Toronto, Canada June 24-28, 2002.

[2] Holz, J., Directed Studies Paper, "Investigation of an Athermal, Refracting Telescope," August 14, 2002.

Contact: Jonathan A. R. Rall, Jonathan.A.Rall@nasa.gov

Laser Technology R&D

Vegetation Canopy Lidar: VCL Laser Transmitter Development

Work on the Vegetation Canopy Lidar Laser Transmitter (VCL LT), has concentrated on increasing reliability, damage risk reduction and lifetesting. Furthermore, the preparation of clean room assembly laboratories for the LTs and developing semi-autonomous data systems for the lasers during assembly has been pursued. Most recently, our work has centered on a VCL Breadboard model of the Laser Transmitter (VCL BB) in order to identify a micro-damage problem with the AR (anti-reflection) coated surface of the laser slabs. This damage issue, has been resolved and the "trigger" set of conditions have been replicated on the BB. Additionally, the High Efficiency Laser Transmitter (HELT), developed by the American University (AU) team, has been run for > $3x10^9$ shots continuously without damage. This proves the viability of the unstable resonator design for long, unattended operation in space. Finally, a diode-based, single frequency seed laser centered at 1064 nm is under development under an Earth Science Technology Office (ESTO) charter.

VCL Laser Transmitter Research and Development

Slab Micro-burns Investigation

Having solved the primary problems with the laser, we discovered that a LT in the process of being constructed would still exhibit a gradual degradation of power. During our troubleshooting effort, it was discovered that small micro-burns, some even < 1 μm in diameter, could be seen on the AR (antireflection) coating on the laser slab. Figure 16 is a photograph of typical micro-burns on a Nd:YAG slab AR surface, magnified at 100X.

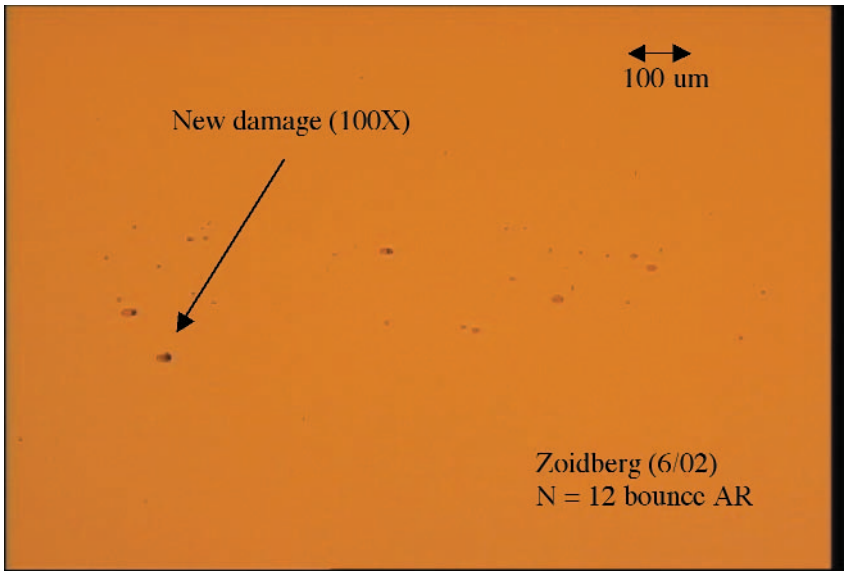

Figure 16: Sample micro-burns on Nd:YAG slab AR surface.

The micro-burns are very small, about 1 μm - 10 μm in diameter and were found in narrow lines, approximately on centerline of the laser beam at the bounce points on the AR coating of the zig-zag slab. The spots are much smaller than the laser beam spot size at the bounce points and propagate (increase) in number and eventually cause a slab to fail. Almost every type of known damage mechanism was thoroughly studied; including contamination, coating quality, coating material, surface quality, surface microfractures, longitudinal mode beating, small scale self focusing,

and others. Each of these potential causes were evaluated and eliminated.

Based on results from a laser simulation software package, GLAD, clipping effects were ruled out, another possible damage trigger, since no effect in the beam profiles or wavefronts were observed. In order to evaluate the intensity fluences, it would be necessary either to work with the LT optical bench outside of the flight laser box or to assemble a laboratory version of the VCL LT. We chose to set-up a breadboard version in a laser R&D laboratory as it provided much more flexibility. In order to accurately quantify any findings and apply them to the LT's, an exact optical replica was made with the breadboard using flight optics, flight optic mounts, and their respective positions.

VCL BB Studies

Studies with the VCL BB were carried out over a period of 6 months. After each change in the cavity parameters, the laser was run at full power for over 16 hours (> 15 million shots) to produce a single data point on performance and damage rate. The slab was inspected and documented. Evidence of micro-burns could be found with an illuminated microscope that employs an encoded translation stage for repeatable inspection precision. In small 1 cm steps, the oscillator cavity was reduced from HELT's configuration of 41cm to the VCL LT fixed length of 37cm. The pump lens to laser diode array (LDA) distance was then changed in several steps as small as +/- 0.001". Figure 17 shows the results of this head variation study.

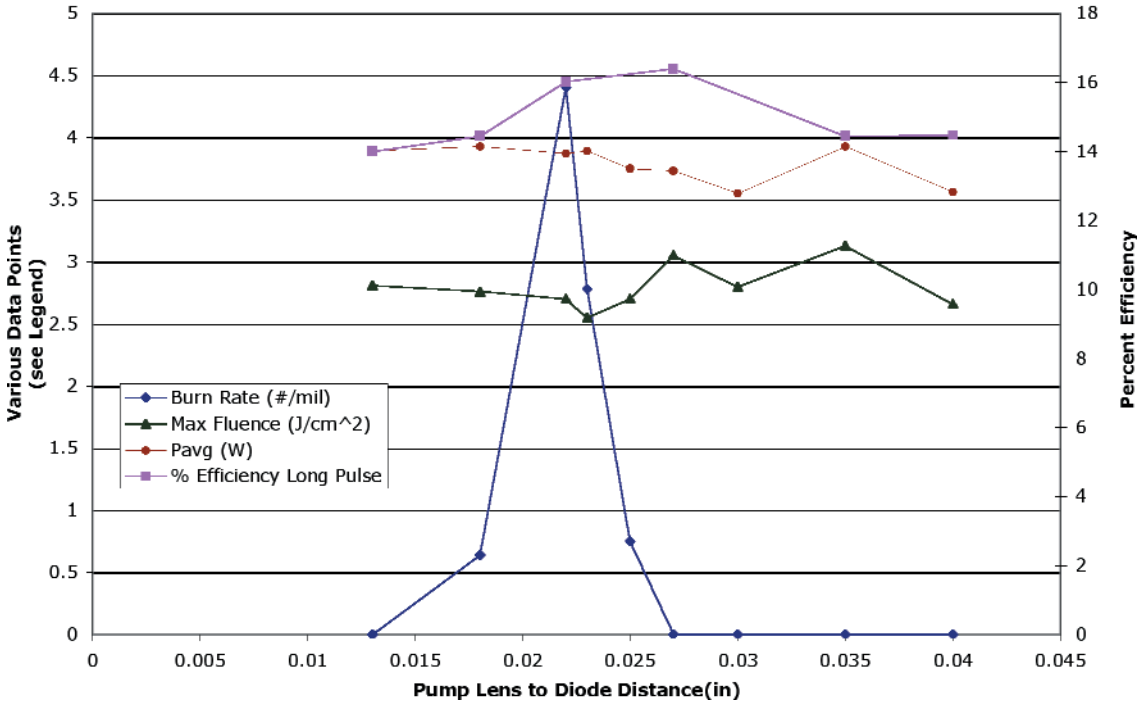

Figure 17. VCL Breadboard Burn Rate Data

Nd:YAG slab damage was present with 4 positions of this pump lens sweep. Upon each of these inspections the total number of new burn locations were cataloged and counted to generate the burn rate plot.

The burn rate vs. pump lens to LDA distance peaks at 0.022" LDA – pump lens spacing. The other data on the graph show that the cavity fluence and optical efficiency change only a small

amount as a function of the pump lens to LDA distance. The cavity loss was adjusted prior to Q-switching in order to provide constant average powers over the course of this experiment. For this reason the efficiency is measured prior to each adjustment. Optical ray trace modeling of the shape and distribution of the pump energy in the slab as a function of the pump lens to LDA distance has been performed in order to identify any correlations with the measured damage peak. Peaking behavior in the pump intensity has been found in models where small filamentary thermal lenses can be produced with individual LDA beams overlapping in the media. It is hypothesized that this effect acts as a damage "trigger" in side pumped head designs. Further work is underway to determine the operational margins in the non-damage settings for this configuration. Figures 18a and 18b show the unfolded and folded assemblies of the VCL BB.

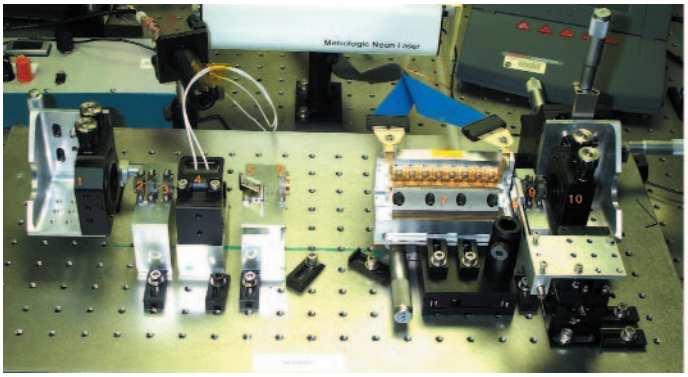

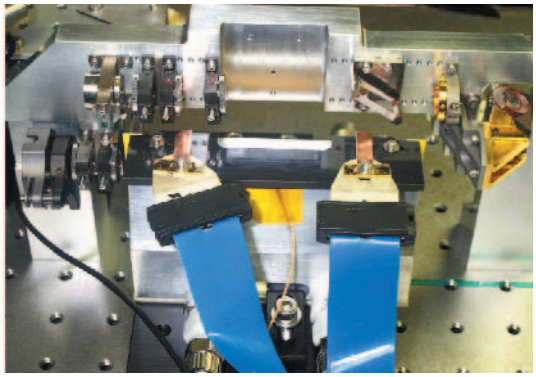

Figure 18a. (at left) Unfolded VCL BB using flight optics, mounts and relative positions (end mirror mounts not shown). Figure 18b. (at right) Folded VCL BB, Q-switch removed, including flight retro.

Final plans for the VCL BB uses a custom optical bench designed to incorporate the 180-degree beam turning "internal-retro". This configuration will be used to find a final optical prescription to be employed in the VCL LT design.

High Efficiency Laser Transmitter (HELT): VCL Lifetest

Features of the HELT laser include an unstable resonator cavity with a Gaussian reflective output coupler designed with the aid of the unstable resonator theory of M. Morin of the Canadian Optics Institute. HELT's pump head is conductively cooled with an optimized design for collimating the pump diode radiation into the zig-zag slab. The VCL BB laser discussed earlier has a head based on this design. The schematic of the basic HELT optical layout is essentially the same as for VCL BB, as this design was adapted by the VCL laser. A near-Brewster cut zig-zag slab is side pumped by 7 four -bar diode arrays of 60 W per bar at up to 70 A drive current.

The unstable resonator consists of an R= 2.5 m concave high reflector (HR) mirror and an R = -2.37 m output coupler. The output coupler is a GRM (graded reflectivity mirror) with a Gaussian reflectivity profile of center reflectivity 63% and $1/e^2$ beam waist of 1.12 mm. Paraxia analysis of this resonator gives beam waists of 1.29 mm and 1.26 mm on the GRM and HR, respectively. The waist in the presence of the slab will be somewhat different due to aperture effects. The geometrical magnification is 1.27 and the total magnification (including diffraction) is 1.40. This magnification is sufficient to reduce the 2nd order mode strength by 50% relative to the TEMoo mode. Further discrimination against higher order modes is provided by the GRM. A thermal lens created in the pump-stripe-dimension of the slab is compensated for by a cylindrical lens of focal length f = -65 cm.

The design of the pump head is significantly different than the VCL LTs. It incorporates 7 four-bar LDAs as compared to VCL (&VCL BB) which have 8 three-bar arrays. Each array is 10 mm

long and the distance between the bars is ~ 0.4 mm. The HELT arrays have a 34% greater emitting area than the VCL head design. Consequently the VCL pump diode illumination is ~ 30% greater in intensity before being collimated with the cylindrical pump lens. The AR coatings on the HELT slab receives lower pump irradiance and pumps a larger volume of the slab for the same input energy. This creates a broader region of inversion density in the slab, promotes a larger lasing beam, and therby reduces the risk of damage from beam irregularities, both spatial and temporal.

A continuous operation lifetest was initiated with the HELT laser in July 2002 in order to determine long term reliability for this design. All operating specifications, such as LDA current, temperature and repetition rate, were held constant and the performance was monitored. Results of this test are illustrated in Figure 4. The run started with 15 mJ of output pulse energy and ended above the end of life requirement of 10 mJ after 2.3 billion laser shots (or one year of operation). The gradual energy loss shown in figure 4 is due to the typical pump diode degradation.

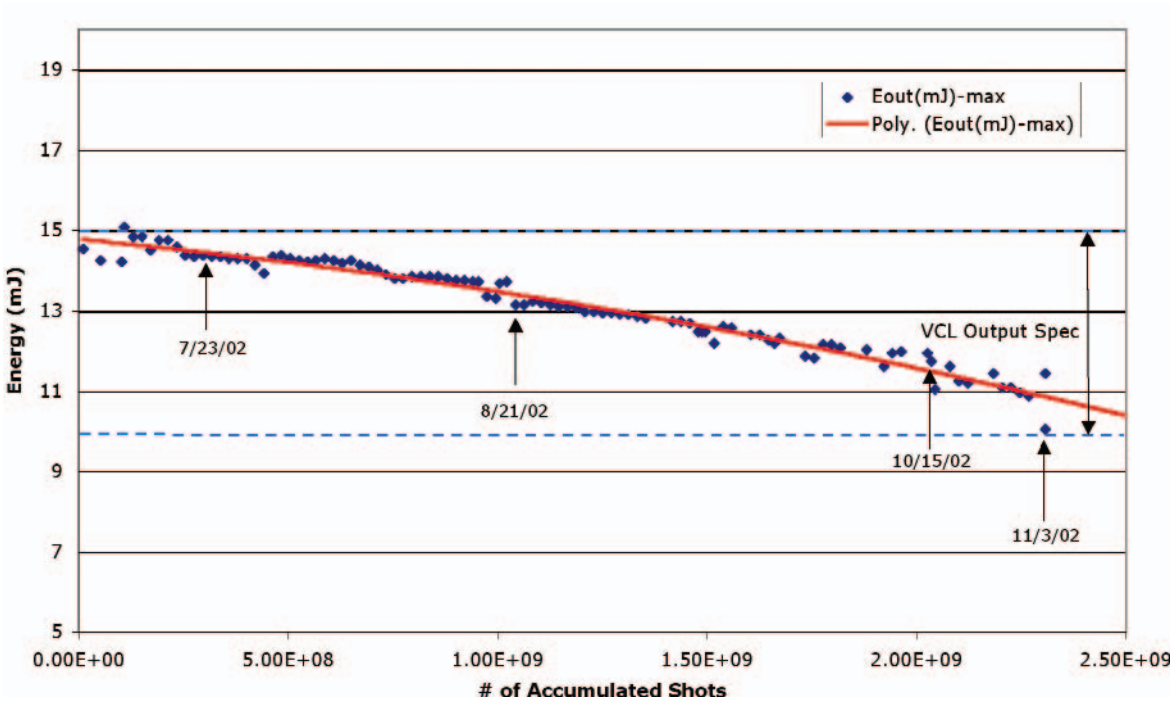

Figure 19. HELT Pulse Energy.

The slab was removed on 7/23/02, 8/21/02, 10/11/02, and 11/3/02 for inspection and no damage was ever found, even under 600x power magnification. The absence of optical damage for a flight laser of this energy and beam quality which has managed a "shot lifetime" of > $2x10^9$ shots is unprecedented. Further, this laser was operated in a normal R&D lab environment, without the benefit of clean room air flow. HELT's LDA pump pulse width has been stepped up from 89us to 105us to increase the pulse energy, and will run for another 2.3 billion shots. As of 01/25/03 HELT has surpassed 3 x 10^9 shots and it should reach 5 x 10^9 shots in April 2003.

Contact: Barry Coyle, Donald.B.Coyle@nasa.gov

Diode Based Single Frequency 1064 nm Laser for Seeding High Power Nd:YAG Lasers

A compact, robust micro laser, wavelength stabilized to 1064.1 nm for use in optically seeding high power Nd:YAG lasers for space lidar applications is under development. Seeding reduces longitudinal mode beating which can damage the optics in a high power laser cavity, greatly reducing its lifetime. The concept of the seed laser is based on stabilizing the output of a standard Fabry-Perot semiconductor laser using optical feedback from a Bragg grating embedded in a KTP waveguide. This design is a proprietary technique developed by AdvR Inc. of Bozeman, MT, the company performing most of the development work. This micro laser is designed as a smaller, more efficient, more robust, less costly replacement for the NPRO (non-planar ring oscillator) Nd:YAG lasers currently used for seeding. The main advantages of a diode based seed laser over the diode pumped NPRO is it requires less components, is inherently more efficient and therefore could potentially cost less.

Brief review and description of progress:

Three of four primary milestones listed have been met in FY02; (1) T\the semiconductor lasers that meet specifications and lifetime have been procured and tested, (2) the KTP Bragg waveguides that will stabilize the semiconductor laser at the proper wavelength for seeding have been fabricated, and (3) a prototype package of the Bragg stabilized laser was delivered to GSFC for seeding experiments. The work is on track for FY03's main task, and 4th milestone, which is to deliver a prototype seed laser ready for vibration and thermal-vac testing by October 2003. This system will come complete with feedback circuitry, fully characterized performance data over temperature, and be optically isolated.

The seeding experiments with the first delivered prototype were successfully performed with the HELT lifetest laser. An improvement in packaging is underway in order to reduce the thermal and mechanical stresses, while retaining ease of alignment. Figure 20 shows the prototype unit prior to assembly.

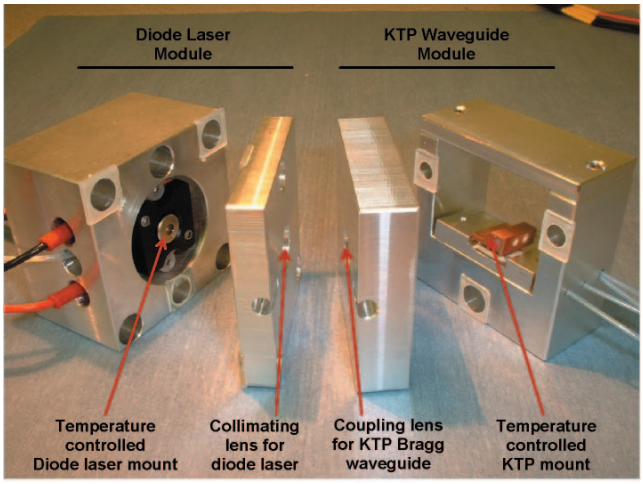

Figure 20. Prototype components of diode seed laser. Each "slice" is approximately 2 inches square. This unit was used to seed HELT lifetest laser in Feb. 2003.

The first delivered prototype package works well in the lab and, to date, has proven to be very temperature insensitive. This compact design is the first effort to house the KTP Bragg stabilized laser in a sealed package with no adjustment knobs for optimum stability. The components are held in aluminum mounts that can be aligned and fixed into place using UV cure epoxy.

Prior to our seed test, the first prototype laser had been running continuously (CW) for a lifetest-for over 50 days. Output power, center wavelength and side mode suppression of the laser was monitored over time and exhibited little or no degradation. A heterodyne technique was used for a high resolution linewidth measurement where two nearly identical lasers are co-aligned and the resultant beat frequency is recorded. Figure 21 shows a measured linewidth of 400 kHz for each laser.

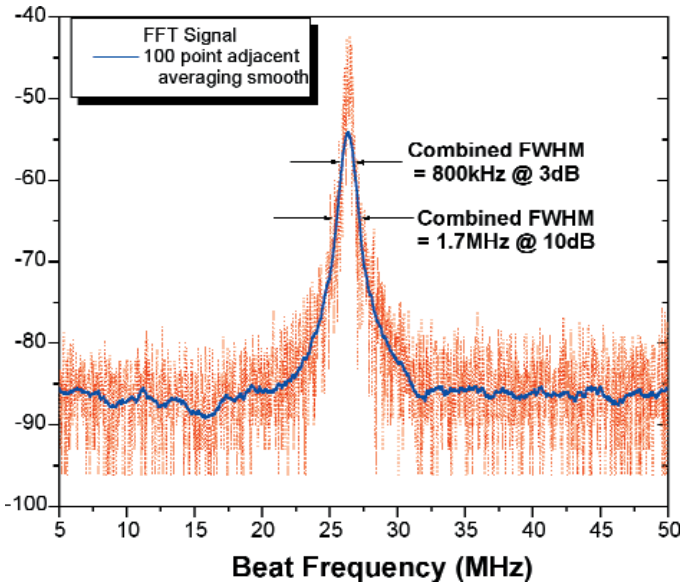

Figure 21. Measured 400 kHz linewidth (800 kHz/2) of 2 identical KTP tuned seed lasers.

Thermal stability of the unit was excellent and no external feedback, thermal, diode drive current, nor KTP voltage was needed to hold seed. The seeding "link" was held continuously for over 5 hours, until we began diode thermal sweeps for characterization purposes. Based on this effort's recent progress, a successful delivery of a flight qualifiable design is expected to be completed by October 2004.

Contact: Barry Coyle, barry@cornfed.gsfc.nasa.gov

One Micron Testbed Program: Laser Risk Reduction

Computer Modeling: Vegetation Canopy Lidar (VCL)

The VCL laser utilizes a Nd^{+3}:YAG zig-zag slab geometry where pump light is coupled into the gain medium through use of a cylindrical undoped YAG lens. Questions arose regarding the distribution of pump light in the slab and if it might be related to optical damage intermittently observed on the slab coatings. To address this issue, the diode array-lens-slab system was modeled using the OptiCAD ray-tracing software. This software not only allows for the design and modeling of optical systems with user-defined individual optical components, but also provides capabilities for the custom design of light sources, including laser diode array (LDA) bars with adjustable performance parameters. Results for the cross-sectional slab pump light distribution for the VCL laser are shown in Figures 22(a) and 22(b) for two different LDA-to-lens distances.

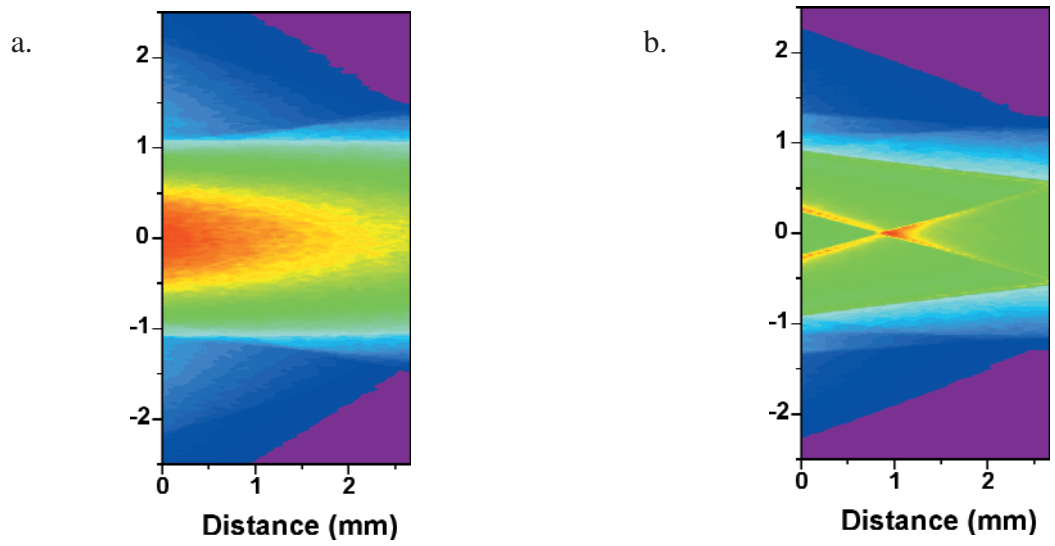

Figure 22: Absorbed energy distribution for diode-to-lens distances of (a) .018" and (b) .035".

At the shorter LDA-to-lens distance, the pump light takes a smooth Gaussian profile across the slab width; however, increasing this distance by only 0.017" (0.43 mm) results in an intraslab focal point roughly 1 mm from the slab input face. Since it has been found that the optical damage observed in VCL is strongly dependent on the position of the pump lens, it may be that such intraslab pump beam focusing plays a significant role. More experimental work is currently underway to examine this possibility.

Another issue with the VCL laser that required attention was possible aperture effects of the intracavity beam by optical components, resulting in the introduction of diffraction rings to the cavity laser mode. To examine this possibility, a code was developed for the physical optics software package GLAD, capable of predicting the transverse cavity mode as well as the phase front of the beam at any point in the oscillator. Figure 23(a) and 23(b) show results for the cavity mode and beam phase front at the slab face. These results indicate that beam clipping at the slab faces does not occur to any significant degree, suggesting diffraction effects are not a likely source of optical damage.

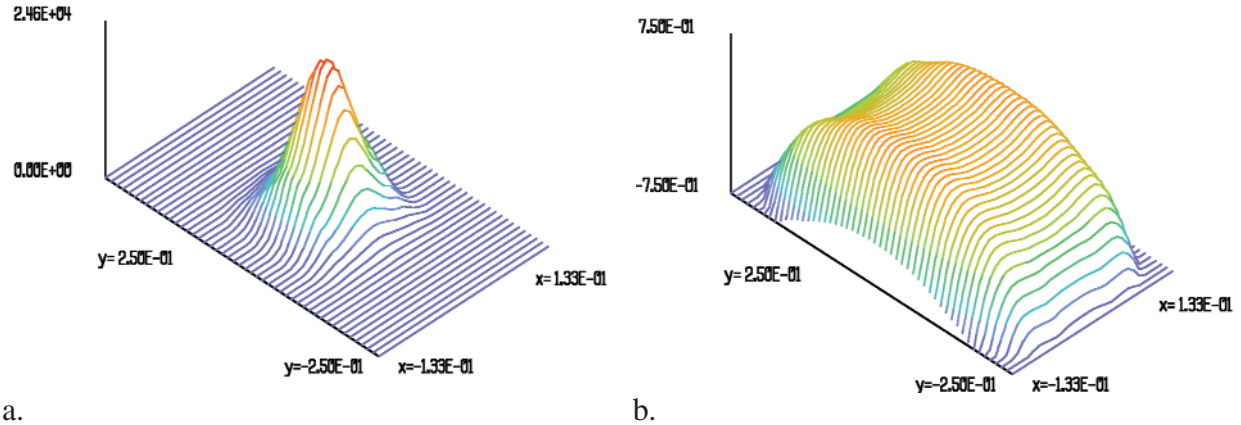

Figure 23: (a) Mode structure and (b) phase front at slab face.

1 μ_ Test Bed

The ability to predict such factors as mode structure, phase distortion, and beam divergence is crucial to the design and optimization of laser systems for the Laser Risk Reduction program. In the interest of testing the accuracy of current modeling methods, computer models for well-characterized oscillators were constructed and matched against empirical data. Two such oscillators chosen for this testing were the MLA and GLAS lasers.

MLA

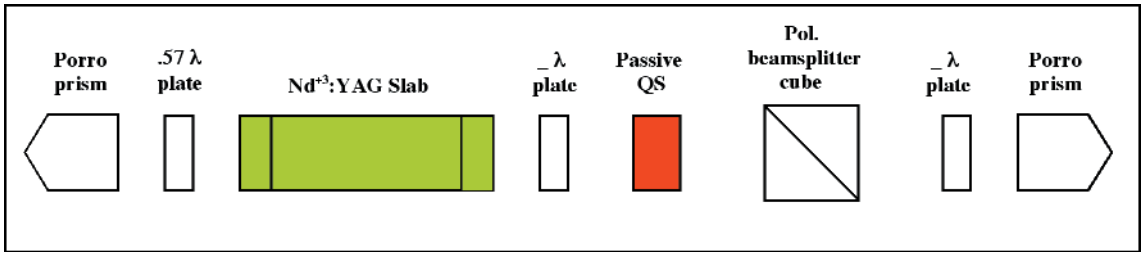

Figure 24: Basic layout of the MLA oscillator.

The quantities of interest for the MLA laser, shown in Figure 24, are the pump light distribution in the slab, intracavity and far-field mode profiles, and beam divergences. First, the distribution of pump light in the slab was investigated. MLA relies on a simple proximity-coupled pump arrangement rather than a pump lens system as in VCL. The cross-section of the OptiCAD-modeled distribution of pump energy for the MLA laser is shown in Figure 25 below:

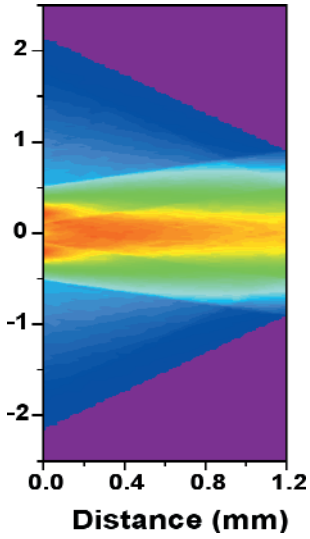

Figure 25: Pump light distribution in MLA slab.

The simulated pump light distribution was then used in a GLAD model to estimate the size and divergences of the output beam. Comparisons of the measured and modeled output beam diameters in the x- and y-dimensions versus distance are shown in Figures 26(a) and 26(b), respectively:

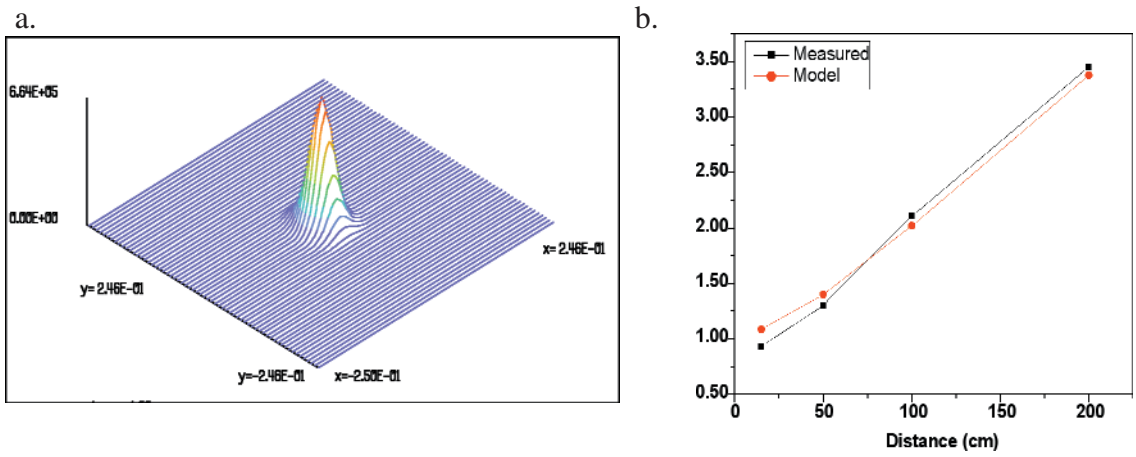

Figure 26: Modeled and measured beam diameters vs. distance for (a) x-dimension and (b) y-dimension.

In addition to providing reliable estimation of the output beam diameter for the MLA oscillator, the GLAD model predicts the x- and y-divergences to be 1.77 mR and 1.79 mR, respectively, as compared to measured values of 1.72 mR for both dimensions.

GLAS

GLAS is another compact, well-characterized passively Q-switched oscillator that provided an opportunity to assay modeling techniques. This laser, illustrated in Figure 27, utilizes a zig-zag slab identical to MLA's, and also makes use of Cr+4:YAG as the saturable absorber material. The major difference between the two systems is that the stimulated radiation is confined in the cavity with a flat 60% output coupler and a 2.5 m HR mirror rather than crossed Porro prisms.

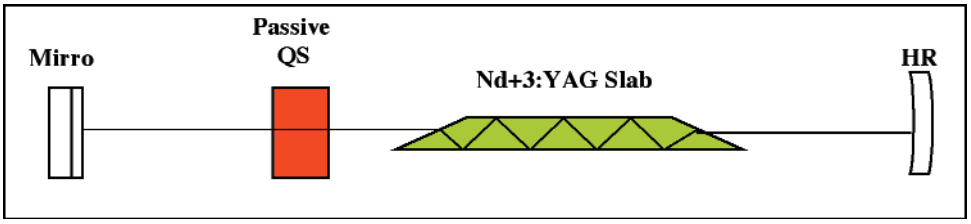

Figure 27: Basic layout of GLAS laser oscillator (no amps shown).

Parameters such as cavity length, pump power, saturable absorber concentration, etc., were estimated from published literature as well as GSFC GLAS documentation and entered into a GLAD code. As was done for MLA, the inversion density distribution in the slab was estimated using OptiCAD. The code calculated ~0.8 mm for the intraslab mode diameter, closely matching the reported value. The model also predicted an output pulse energy of 1.24 mJ as compared to the reported 1.5 mJ. However, the predicted 2.4-3.0 ns pulsewidth underestimates the experimental value of ~4 ns. Example data from the GLAD code is shown in figures 28(a) and 28(b):

a. b.

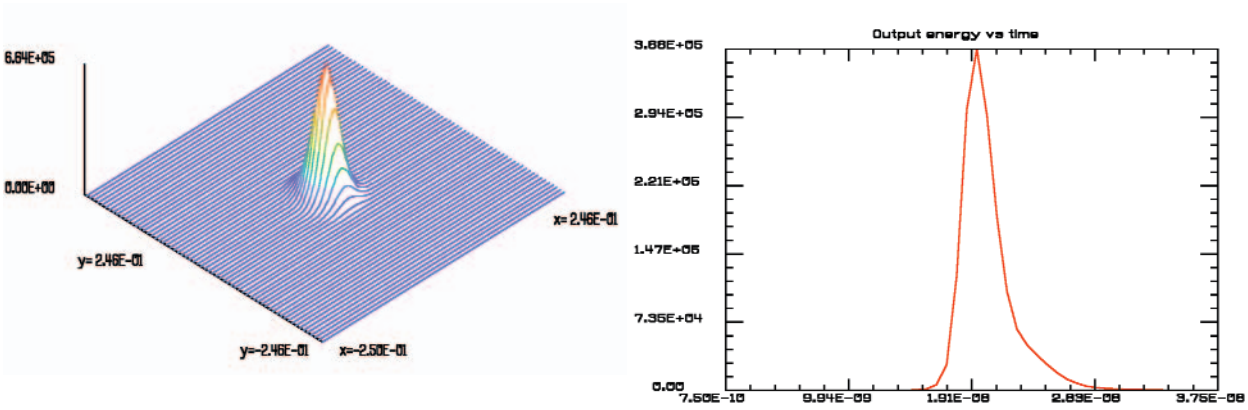

Figure 28: (a) Predicted near-field mode structure and (b) output pulse shape for GLAS laser.

Contact: Barry Coyle, Donald.B.Coyle@nasa.gov

Fiber Amplifier Power Scaling/Frequency Doubling Effort

The Fiber Amplifier Power Scaling/Frequency Doubling effort is a laboratory research project to demonstrate the feasibility of using fiber optic amplifiers as laser sources/transmitters for a variety of Earth science applications. Fiber amplifier-based lasers have many potential advantages for use in space due to their compact, rugged and highly efficient nature. They can address a broad wavelength region in the NIR that can be extended into the visible region using nonlinear, second harmonic generation (i.e. frequency doubling). Atmospheric CO_2 and O_2 can be actively sensed with lasers operating at 1572 nm and 761 nm respectively. Vegetation Index (i.e. chlorophyll content of vegetation) can be estimated using two lasers operating at 660 nm and 785 nm and taking the ratio of reflected laser energy. Currently there are no space-qualified, high power lasers at these wavelengths. Rare earth doped (Ytterbium & Erbium), high power (5-10 W CW) fiber amplifiers are commercially available telecom products.

Literature and web searches were conducted to identify as many academic institutions and industry vendors as possible to accurately establish the state of the art (i.e. Technology Readiness Level or TRL) of high power (10 W CW and >300 kW pulsed) fiber amplifier work and efficient (>50%) non-phase matched second harmonic generation (SHG) of these devices. Research conducted at the Imperial College of London, UK has demonstrated efficient frequency doubling (>40%) of Yb-doped fiber amps to the 3-6 Watt level. More recently, research at the Naval Research Lab in Washington, D.C. has demonstrated pulsed fiber amplifiers at 1064 nm producing 300-kW pulses.

A conceptual design was developed of a frequency-doubled fiber amplifier system based on knowledge gathered from academia and industry. Two parallel approaches have been identified: Rare-earth doped (e.g. Ytterbium (Yb) and Erbium (Er)) fiber amplifiers for "fixed" wavelength (1.0 μm and 1.5 μm) systems and Raman amplification in standard SMF-28 transport fiber for "custom" wavelengths (1.2-1.6 μm). Phase matched SHG was deemed too complicated to ever be elevated to an appropriate TRL for space applications. Therefore, non-critical, quasi-phase matched SHG using periodically-poled non-linear optical crystals was the selected approach. A relatively new material, periodically-poled KTP (PPKTP) was chosen because it offers high conversion efficiency (>50%) and ruggedness as compared to Lithium Niobate.

All the major equipment was procured in FY02 and we will begin assembling the initial demon-

stration experiment in the 2nd quarter of FY03. This will include characterizing the performance of the Er/Yb doped fiber amp with both a CW seed and pulsed seed source and at both the fundamental wavelength, 1570 nm, and frequency doubled to 785 nm. A similar demonstration/characterization will be performed with the 40 dBm Raman Amplifier. Other work that we will address this year includes identifying non-linear processes such as Stimulated Brillouin Scattering (SBS) and Stimulated Raman Scattering (SRS) which become problematic with short (e.g. nanosecond) pulses and high peak powers. Future investigations will explore different methods to mitigate these technical hurdles while ensuring good doubling efficiency and narrow linewidth operation.

References:

[1] Champert, P.A., S.V. Popov, & J.R. Taylor, "3.5 W frequency-doubled fiber-based laser source at 772 nm," Applied Physics Letters, Vol 78, No 17, April 23, 2001.

[2] Di Teodoro F., J.P. Koplow, S.W. Moore, & D.A.V. Kliner, " Diffraction-Limited, 300-kW peak-power pulses from a coiled multimode fiber amplifier, Optics Letters, Vol 27, No. 7, April 1, 2002.

Contact: Jonathan A. R. Rall, Jonathan.A.Rall@nasa.gov

Laser Sounder Technique for Remotely Measuring Atmospheric CO_2 Concentrations

Accurate measurements of tropospheric CO_2 abundance with global-coverage, 300 km spatial and monthly temporal resolution are needed to quantify processes that regulate CO_2 storage by the land and ocean. We are investigating the feasibility of a satellite-borne laser-sounding instrument that would meet these requirements. The laser sounder approach uses the differential absorption technique to accurately measure the atmospheric column abundance. We propose to use three separate laser transmitters to permit simultaneous measurement of 1) CO_2 - at 1570 nm 2) O_2 - at 770 nm and 3) aerosol backscatter - at 1064 nm - in the same atmospheric path. This method greatly reduces the major error sources including interference from other trace gas species (e.g. H_2O), variability in dry air density caused by pressure or topographic changes, the effects of clouds and aerosols in the path and diurnal biases in CO_2 concentration. The laser sounder technique uses the strong reflection from the Earth's surface. This greatly enhances the system feasibility for near term space deployment.

We choose to work at the CO_2 overtone band at 1570 nm that falls within the telecommunication L-band and at 1540 nm (the O_2 A-band at 770 nm =1540 nm/2) in the telecommunication C-band in order to leverage the world-wide industry investment in the associated laser and electro-optic technology. This includes single-frequency DFB laser diodes and high optical power (>10 W average) erbium fiber amplifiers recently space qualified by Lucent.

The active sounding technique has advantages over passive spectrometers in its high (MHz) spectral resolution and stability, the ability to measure at night and in dim-light, a narrow measurement swath, and the ability to simultaneously detect and exclude measurements with clouds or aerosols in the path. For space, the concept is a lidar measuring at nadir in sun-synchronous orbit. Using dawn and dusk measurements make it possible to sample the diurnal variations in CO_2 mixing ratios in the lower troposphere. A 1-m telescope is used as the receiver for all wavelengths. When averaging over 50 seconds, a SNR of ~1500 is achievable for each atmospheric constituent at each on- and off-line measurement. Such a mission can furnish global maps of the lower tropospheric CO_2 column abundance at dawn and dusk. Global coverage with an accuracy of a few ppm with a spatial resolution of ~ 50,000 sq. km appears achievable each month.

Under NASA's ESTO ATI (Earth Science Technology Office Advanced Technology Initiative) program support, we have demonstrated key elements of the CO_2 measurement technique, laser transmitter, photon counting detector. These include measurements of line shapes for CO_2 in an absorption cell using the fiber amplifier transmitter, and measurements at 1570 nm with SNRs of > 500 using a PMT detector. Recently we have made stable CO_2 absorption measurements over a 205m-long open horizontal path using our breadboard sounder instrument [± 1.7% (7 ppm) accuracy with 10 s averaging time], and have obtained good agreement with HITRAN predictions and with simultaneous measurements from an in-situ CO_2 analyzer over several hours.

In addition to this system effort, we have initiated key component development efforts for 1) high-peak-power single-frequency fiber-amplifiers with reduced Stimulated-Brillouin-Scattering (GSFC Internal R&D funds), 2) InGaAs avalanche photodiode photon counting detectors (NASA's ESTO Laser Risk Reduction funds) 3) frequency-doubled erbium-fiber-amplifier based laser transmitters (GSFC Internal R&D).

Contact: James Abshire, James.B.Abshire@nasa.gov

Spaceborne Imaging Laser Altimetry Mission Concept and Technology Development

The Laser Remote Sensing Branch at GSFC is investigating various techniques for implementing an LVIS-like, wide-swath, full-waveform imaging laser altimeter in space. This instrument will enable high accuracy, high resolution full Earth mapping. A concept for a full-Earth imaging laser altimeter mission is being developed for possible launch in 5-10 years. The goal of this mission would be to completely map the topography and vegetation structure of the entire land surface of the Earth including topography beneath dense vegetation, all at < 10 m horizontal resolution. The concept utilizes extremely high rep-rate lasers (75 kHz), a streaming waveform digitizer system for recording the range to the surface and the vertical structure of each pixel, and a novel high-speed, highly accurate laser scanning system. The data set from this system would represent 2 orders of magnitude improvement in vertical accuracy (~ 10 cm), and 1-2 orders of magnitude improvement in horizontal resolution (< 10 m) over existing data. The waveform-based measurement is a proven technology developed specifically for vegetation penetration and novel topographic change detection (including beneath vegetation).

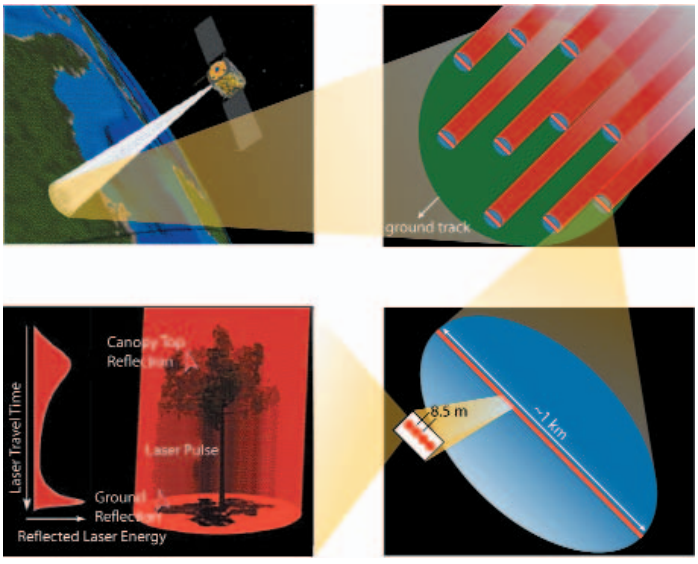

Figure 29. The graphic below illustrates the full-Earth imaging lidar concept. Starting at the upper left and going counter-clockwise: 1) View of the spacecraft nadir swath encompassing a 10 km diameter field-of-view (FOV). 2) 10 km FOV segmented into ten, 1 km mini-swaths. 3) Individual 1km mini-swath consisting of ~120 discrete laser footprints that will be scanned at a high rate across the nadir track of the spacecraft. 4) Last is an illustration of the full return-waveform concept showing the full illumination of the area within each footprint and the resulting return echo that fully characterizes the vertical structure of its topography and vegetation

Contact: Bryan Blair, James.B.Blair@nasa.gov

Investigation of Bose-Einstein Condensates for Advanced Gravity Gradiometer Designs

Measurements of the gradient in the gravity field of the Earth from orbit provides a powerful investigative tool for global geophysical effects. Deep ocean currents, the seasonal bulk redistribution of the atmosphere, and water storage and transport (i.e. in underground aquifers and deep ice sheets) are some of the many phenomena that produce gravitational effects that can be studied with orbiting gradiometers.

Recent developments in ultra-cold matter have resulted in the creation of a new state of matter, Bose-Einstein condensates. These condensates are small clouds of gas at nanoKelvin temperatures. These temperatures can be reached without cryogenics by the clever use of lasers. At these temperatures the atoms in the gas cloud display interference patterns which are strongly influenced by gravity. A brief investigation has concluded that a matter interferometer based on these condensates may permit the construction of gravity sensors orders of magnitude more sensitive than any prior technique.

Without the need for cryogenics it is possible to envisage a satellite-based gradiometer that could have a long lifetime. Such an instrument would permit Earth studies over a multi-year baseline.

This work specifically targets the design of an orbital (zero-g) instrument that might enable a future gravity sensing mission. The first objective is to analyze the potential performance of new, in-house, gravity gradiometer designs via computer simulations. Next is to identify the geophysical phenomena that would become observable with the increased sensitivity of these cold-atom interferometer designs. These studies will be used to seed new instrument/mission proposals.

Key technology elements needed to establish a starting point for Goddard research into these condensates are being identified. The goal of this effort is to investigate the design of spaceflight versions of the existing laboratory subsystem elements such as atomic vapor ovens, magneto-optical traps, and evanescent-wave atom mirrors.

Contact: David Skillman, David.R.Skillman@nasa.gov

Satellite Laser Ranging

NASA Satellite Laser Ranging (SLR) Network

Satellite Laser Ranging (SLR) is a fundamental measurement technique used by the NASA Space Geodesy Program to support both national and international programs in Earth dynamics, ocean and ice surface altimetry, navigation and positioning, and technology development. NASA built the five trailer-based Mobile Laser Ranging Stations (MOBLAS) that have remained in operation at fixed sites for over fifteen years. Two highly compact Transportable Laser Ranging Systems (TLRS), built by NASA, also remain in operations. The University of Hawaii and the University of Texas continue to operate the two high performing Observatory SLR systems at their respective Universities. The University of Texas system also has lunar ranging capability.

NASA has continued its successful partnerships with the Australian Surveying & Land Information Group (AUSLIG) in Yarragadee, Australia (MOBLAS-5); the South African National Research Foundation/Hartelbeesthoek Radio Astronomical Observatory (HRAO) in Hartelbeesthoek, South Africa (MOBLAS-6); and the University of French Polynesia/CNES in Tahiti, French Polynesia (MOBLAS-8). Under these partnerships, NASA continues to provide the SLR system, training, engineering support, and spare parts to maintain operations. The host country provides the site, local infrastructure, and the operating crew. NASA has begun discussing a partnership agreement with the Indian Space Research Organization (ISRO) located in Bangalore, India for the operations of TLRS-4.

The NASA SLR Network has been fully operational in the field for over twenty years. During this time, the Network has seen many modifications and upgrades to maintain system operations and more importantly, to increase data quantity and quality. Through a declining budget, NASA continues to ensure system operations and performance are maintained at the highest level. During the last two years, the MOBLAS, TLRS, MLRS (University of Texas SLR system), and HOLLAS (University of Hawaii SLR system) have received both hardware and software changes to maintain and enhance system operations. Upgrades were made to the timing subsystem, the receiver subsystem, the laser subsystem, the communications subsystem, the mount subsystem, and the processing software for the NASA SLR Network.

In summary, the NASA Network still consists of nine NASA operated, partner operated and University operated stations covering North America, the west coast of South America, the Pacific, South Africa, and Western Australia. The NASA SLR Network continues to provide over 40% of the total data volume in the International Laser Ranging Service (ILRS) as well as the most precise sub-cm accuracy ranging data.

Table 4. NASA Satellite Laser Ranging Network

Location	SLR System	Operating Agency
Monument Peak, California	MOBLAS-4	Mission Contractor (HTSI)
Greenbelt, Maryland	MOBLAS-7	Mission Contractor (HTSI)
Mount Haleakala, Maui, Hawaii	HOLLAS	University of Hawaii
Fort Davis, Texas	MLRS	University of Texas at Austin
Arequipa, Peru	TLRS-3	Universidad Nacional de San Agustin
Yarragadee, Australia	MOBLAS-5	Australian Surveying & Land Information Group
Hartebeesthoek, South Africa	MOBLAS-6	National Research Foundation
Tahiti, French Polynesia	MOBLAS-8	University of French Polynesia/CNES
Bangalore, India *	TLRS-4	Indian Space Research Organization (ISRO)

* Preliminary Discussions underway

Contact: David Carter, David.L.Carter@nasa.gov

International Laser Ranging Service

The ILRS was established in 1998 as an official service of the International Association for Geodesy (IAG). The ILRS collects, merges, analyzes, archives, and distributes Satellite Laser ranging (SLR) and Lunar Laser Ranging (LLR) observation data sets of sufficient accuracy to satisfy the objectives of a wide range of scientific, engineering, and operational applications and experimentation. The basic observable is the precise time-of-flight of an ultrashort laser pulse to and from a satellite, corrected for atmospheric delays. These data sets are used by the ILRS to generate a number of fundamental data products, including: centimeter accuracy satellite ephemerides, Earth orientation parameters, three-dimensional coordinates and velocities of the ILRS tracking stations, time-varying geocenter coordinates, static and time-varying coefficients of the Earth's gravity field, fundamental physical constants, lunar ephemerides and librations, and lunar orientation parameters. As such, the ILRS provides fundamental data to support the International Terrestrial Reference Frame (ITRF) and the International Earth Rotation Service (IERS). The ILRS consists of several operational elements: tracking stations, operational centers, analysis centers, data centers, and a central bureau.

ILRS Governing Board

The Governing Board is responsible for the general direction of the ILRS. It defines official ILRS policy and products, determines satellite tracking priorities, develops standards and procedures, and interacts with other services and organizations. There are sixteen members of the board; elections for the next two-year term of the ILRS Governing Board were held in mid-2002. Table 5 shows the current members of the board.

Table 5. ILRS Governing Board (as of October 2002)

Hermann Drewes	Ex-Officio, CSTG President	Germany
Michael Pearlman	Ex-Officio, Director ILRS Central Bureau	USA
Carey Noll	Ex-Officio, Secretary, ILRS Central Bureau	USA
Werner Gurtner	Appointed, EUROLAS, Governing Board Chairperson	Switzerland
Giuseppe Bianco	Appointed, EUROLAS	Italy
David Carter	Appointed, NASA	USA
Jan McGarry	Appointed, NASA	USA
Ben Greene	Appointed, WPLTN	Australia
Hiroo Kunimori	Appointed, WPLTN, Missions WG Coordinator	Japan
Bob Schutz	Appointed, IERS Representative to ILRS	USA
Graham Appleby	Elected, Analysis Representative	UK
Ron Noomen	Elected, Analysis Representative	The Netherlands
Wolfgang Seemueller	Elected, Data Centers Representative	Germany
Peter Shelus	Elected, Lunar Representative	USA
Georg Kirchner	Elected, At-Large Representative	Austria
Ulrich Schreiber	Elected, At-Large Representative	Germany

Working Groups

The ILRS has established five Working Groups to help formulate policy and provide technical expertise. The Missions Working Group routinely reviews current tracking priorities and campaigns, and develops recommendations on new requests for tracking support. During 2002, the Missions Working Group coordinated support for ADEOS-II (environmental monitoring), GRACE (gravity field studies), JASON (ocean surface topography), and ENVISAT (follow-on to ERS for climate research). In 2002, the Data Formats and Procedures Working Group reviewed the user requirements for SLR full-rate data and established procedures for transmitting and archiving these data as well as processing two-color laser ranging data. This working group continues to sponsor two study groups, one on determining necessary modifications to the current

satellite predictions format and a second on atmospheric refraction models used in SLR analysis. The Networks and Engineering Working Group completed work on gathering system information into consistent site-specific log files and compiled this information into a spreadsheet for ease of use by the analysis community. The Analysis Working Group held two workshops in 2002. These meetings focused on benchmarking and pilot projects designed to assess the current state of the SLR analysis community and eventually develop standard ILRS products such as daily X/Y pole and length-of-day values for the IERS. During 2002 the Signal Processing Ad Hoc Working Group continued to work on improved center-of-mass corrections and signal processing techniques for the many satellites currently tracked by SLR.

Tracking Network

In 2002, three stations were approved by the ILRS Governing Board for membership in the ILRS tracking network: the optical station located at the Naval Research Laboratory in Washington D.C., a system located at the Astronomical Observatory of Ivan Franko National University of Lviv, Ukraine, and the refurbished system at the Communications Research Laboratory in Koganei (near Tokyo), Japan. Furthermore, the TIGO (Transportable Integrated Geodetic Observatory) system became operational in Concepción, Chile in May 2002 and has become a key component of the continued effort to strengthen SLR coverage in the southern hemisphere. The addition of these stations expands the operational ILRS network to over forty systems as shown in Figure 32.

Figure 30. Current ILRS Network

Missions

During 2002, the ILRS provided operational tracking of over thirty targets, including passive geodetic (geodynamics) satellites, Earth remote sensing satellites, navigation satellites, engineering missions, and lunar reflectors. The Governing Board recently approved the tracking of two new missions, ICESat, in support of precise orbit determination (POD) for the altimeter and validation

of the GPS instrument, and the National Polar-orbiting Operational Environmental Satellite System (NPOESS), a 2013 mission, for POD. Four previously approved missions, ADEOS-II, GRACE, JASON, and ENVISAT were launched and successfully tracked by the ILRS network during 2002. Continued tracking of both ADEOS-II and ICESat will be coordinated with the sponsoring agencies because of optical sensitivity of on-board instruments. The METEOR-3M mission requested emergency satellite tracking by the ILRS network due to the failure of the on-board GLONASS receiver to provide sufficient POD for the SAGE-II instrument. The ILRS supported two intensive tracking campaigns in 2002: ETALON and Reflector; tracking priorities for these satellites were elevated in order to increase data yield. Analysts requested additional tracking of the two ETALON satellites in order to study Earth orientation and low order, low degree harmonics of the gravity field. The Reflector satellite was a novel approach to investigate satellite dynamics using a distributed array.

ILRS Central Bureau

The Central Bureau continued development of a new website for the ILRS which became operational in May 2002. In addition to a complete content review, this new website provides easier information retrieval through breadcrumbs and a navigation bar as well as an upgraded search engine. A bibliography of articles relevant to SLR was completed and installed in the website. Staff conducted a thorough review and implementation of site documentation for all stations in the ILRS network. The Central Bureau also coordinated the publication of the 2000 and 2001 editions of the ILRS Annual Report series. A revised brochure highlighting key areas of interest in the ILRS website was compiled and published in September 2002. The central bureau also arranged various meetings of the service and working groups at the April European Geophysical Society (EGS) assembly and the October laser ranging workshop.

Meetings

The ILRS was a co-sponsor, with NASA and the Smithsonian Center for Astrophysics, of the 13th International Workshop on Laser Ranging, held in Washington D.C. during the week of October 7, 2002. The workshop was a very successful venue for the exchange engineering and scientific information with the intent to improve the scientific product of laser ranging. Over 160 colleagues attended the five-day event which covered such topics as scientific achievements, station performance evaluation and operational issues, target design, timing devices, system calibration, atmospheric correction, detectors, technology development, automation and control systems, and advanced systems and techniques.

The 7th and 8th ILRS General Assembly meetings were held in April and October 2002, in conjunction with the EGS Spring Meeting in Nice, France and the 13th International Workshop on Laser Ranging in Washington D.C., respectively. Both meetings were well attended and allowed the ILRS to present current status and obtain feedback on operational issues from the international community. Meetings of the Governing Board and Working Groups were also held during these time periods.

Web site: http://ilrs.gsfc.nasa.gov

Contact: Carey Noll, Carey.E.Noll@nasa.gov

SLR2000 Autonomous Satellite Laser Ranging Station

Next generation NASA Satellite Laser Ranging (SLR) systems will be replications of the SLR2000 system currently under development at the Goddard Geophysical and Astronomical Observatory (GGAO) in Greenbelt, Maryland. The SLR2000 is a fully autonomous, eye-safe, sub-centimeter precision ranging instrument capable of tracking a wide range of cube corner equipped satellites up to 20,000 km altitude. Satellite range is determined by measuring round trip time-of-flight accurate to a few picoseconds, applying system calibration offsets and correcting for atmospheric refraction. Scientific applications include maintenance of terrestrial reference frames, precision orbit determination, geophysics, gravity studies, fundamental physics, and global time transfer. The SLR2000 is operated in an eye -safe fashion by reducing the single pulse energy to 135 mJ per pulse at the exit port while filling the whole 40 cm telescope with the transmit beam. The current NASA Mobile Laser Ranging Stations (MOBLAS) transmit an average power of about 500 mw in making 5 measurements per second. By comparison, the SLR2K has an average transmitted power of only 270 mw. While firing at a 2 KHz rate SLR2K will make 10 to 100 times more range measurements per second than a MOBLAS system. This is accomplished by the efficient use of receive photons in the range measurement in operating at the single photoelectron signal level.

SLR2K SYSTEM PARAMETERS

Laser:	**Diode pumped Nd:YAG**
Fire rate:	**2 KHz**
Pulse Energy:	**135 ujoules/pulse**
Beamwidth:	**10, 40 arcsec (exit port)**
Detector:	**Photek quadrant MCP PMT**
Gain:	**3.E6**
QE:	**13% @ 532 nm**
Active area:	**12 mm diameter**
Image size:	**6 mm**
Receiver:	**4 independent channels**
Field of view:	**10, 40 arcsec**
Discriminator:	**Phillips Scientific 708**
TIU:	**HTSI 1.5 ps Event Timer**
Risley prisms:	**0-30 arcsec point ahead**
T/R Switch:	**Polarization (passive)**
Telescope:	**OSC 40 cm off-axis**
Pointing system:	**Xybion Ax/El gimbal**
Tracking error:	**~ arcsec RMS both axes**
Command rate:	**50 Hertz**

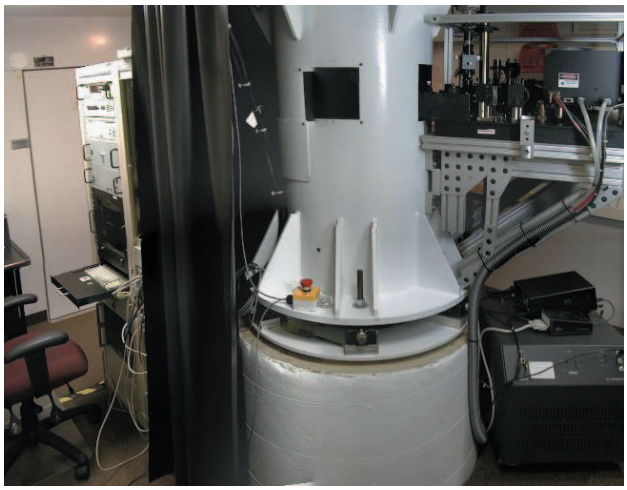

Figure 31. SLR2000 system specifications (left) and photo of the shelter interior (right).

Progress on the SLR2000 project has been held up the past year with two major problems identified and corrected in the 40-cm off-axis telescope. Image quality expected to be better than 2 arcseconds was typically only 18 to 20 arcseconds. This was found to be caused by a shift in the position of the primary mirror in its holding cell. The second problem involved an internal fold mirror of the telescope with insufficient angular adjustment. Both problems have been corrected and work continues on system check out and verification. The laser transceiver table has been installed and optical alignments for both gimbal and telescope are being conducted. Visual star calibrations will begin in early CY03 with visual satellite tracks and laser tracking by the end of CY03.

Contact: Tom Zagwodzki, Thomas.W.Zagwodzki@nasa.gov

Calibration

EOS Calibration

The Earth Observing System (EOS) is a decadal, international multi-satellite program in global remote sensing of the Earth. As such, EOS is and will continue to be the fundamental source of satellite data on the earth and its environment into the 21st century. The overall goal of the EOS mission is to advance the scientific understanding of the entire earth system and its changes on a global scale through the development of a deeper understanding of the components of that system and their interactions. In order to achieve those goals, EOS has and will continue to produce global, long-time series, remote-sensing data sets from multiple instruments on several satellite platforms. The correct interpretation of scientific information from these data sets requires the ability to discriminate between on-orbit changes in the instruments and changes in the earth physical processes being monitored. The ability to make this distinction depends crucially on the calibration of the instruments with respect to a set of recognized physical standards or processes, the careful characterization of the instruments' performance at the subsystem and system levels, the cross-calibration of the instruments, and the post-launch validation of the instruments fundamental radiance and reflectance products.

Code 920.1 provides technical and administrative support to the EOS Project Science Office in the calibration of satellite, airborne, and ground-based instruments. This includes coordinating and participating in satellite instrument reviews, participating in algorithm theoretical basis document (ATBD) reviews, coordinating and participating in measurement assurance programs (MAPS) with the assistance of the National Institute of Science and Technology (NIST), and providing over-arching technical guidance in the EOS lunar photometry project underway at the United State Geological Survey in Flagstaff, Arizona.

Instrument Reviews and Workshops

In 2002, the EOS Calibration program, operating within Code 920.1, participated in and/or coordinated a number EOS instrument and mission-level reviews and workshops. These reviews included the following:

•Solar Radiation and Climate Experiment (SORCE) Instrument Pre-ship Review; Laboratory for Atmospheric and Space Physics; University of Colorado; Boulder, Colorado; February 21-22, 2002.

•High Resolution Dynamics Limb Sounder (HIRDLS) Calibration Working Group Meeting; Oxford University; Oxford, United Kingdom; July 10-11, 2002.

•Solar Radiation and Climate Experiment (SORCE) Observatory Pre-ship Review; Orbital Sciences Corporation; Dulles, Virginia; October 21, 2002.

•Multi-angle Imaging SpectroRadiometer (MISR) Calibration Review; Jet Propulsion Laboratory; Pasadena, California; October 22, 2002.

•Workshop on Satellite Instrument Calibration for Measuring Global Climate Change; University of Maryland; College Park, Maryland; November 12-14, 2002.

Aperture Round-robin and Instrument Measurement Comparison in Support of the Measurement of Total Solar Irradiance

The concept for an aperture area comparison involving representatives from the solar irradiance

measurement community was formulated at the May 2000 Calibration Workshop for the Total Irradiance Monitor (TIM) held at the University of Colorado's Laboratory for Atmospheric and Space Physics (LASP). In 2002, the comparison was initiated and is being coordinated by the National Institute of Standards and Technology (NIST) Optical Technology Division and the EOS Project Science Office at NASA Goddard. The NIST Optical Technology Division has expertise in the metrology of aperture area as applied to radiometry. The goals of the comparison are to provide an independent determination of the area of circular apertures that have heritage with solar irradiance determinations, thus providing a measurement of the reproducibility, and to use this information to evaluate discrepancies in determinations of the solar constant. Participants in the aperture area comparison include the World Meteorological Organization (WMO), the Royal Meteorological Institute of Belgium, the Jet Propulsion Laboratory (JPL), and the Laboratory for Atmospheric and Space Physics (LASP) University of Colorado.

The EOS Calibration program has coordinated discussions on measurement comparisons between the TIM and the Active Cavity Radiometer Irradiance Monitor (ACRIM). The TIM was launched on January 25, 2003 on EOS SORCE. ACRIM instruments have provided a 20 year data record of total solar irradiance measurements. Currently, the ACRIM III instrument launched on December 20, 1999 on EOS ACRIMSAT and the VIRGO suite on SOHO are providing total solar irradiance data. Both the TIM and ACRIM instrument teams agreed that the first and primary comparison of TIM to ACRIM and other TSI-measuring instruments will be on-orbit in mid 2003. The participants also agreed that if those on-orbit comparisons between TIM and ACRIM do not agree to within the ACRIM measurement uncertainty of 0.2%, then ground-based and shuttle-based comparison of the instruments will be warranted. Those comparisons would be coordinated by the EOS Calibration program.

Robotic Lunar Observatory Calibration

The Robotic Lunar Observatory (ROLO) funded by the EOS Project Science Office and located at USGS in Flagstaff, Arizona, has developed a spectral irradiance model of the Moon while accounting for the effects of lunar libration, phase, and spacecraft location. This lunar irradiance model can be used as an effective on-orbit reference to compare current calibrations of orbiting satellite instruments. In an effort to establish an absolute radiometric scale to the ROLO lunar observations, NASA's Code 920.1, NIST, and the University of Arizona have teamed with USGS to fully characterize the ROLO telescope/detector systems. This effort began in early 2002 and will culminate in mid 2003 by using a NIST calibrated collimated source to measure the ROLO small angle scatter and system level radiance response.

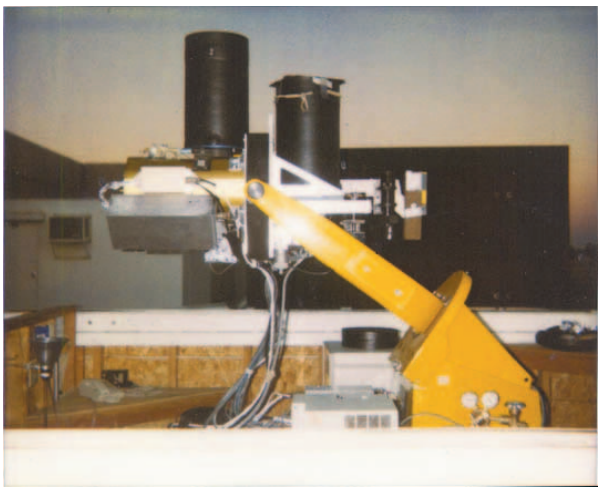

Figure 32. The ROLO visible/near infrared and shortwave infrared telescopes located at USGS in Flagstaff, Arizona.

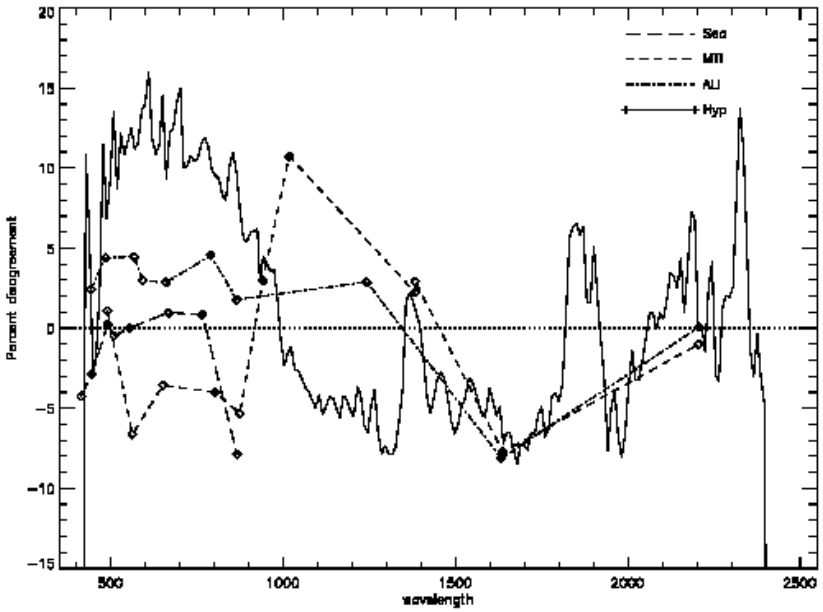

Figure 33. The lunar irradiance model produced by the ROLO project enables the on-orbit calibrations of remote sensing instruments to be compared. The lines on this plot represent the % deviation of the calibration of the Sea-viewing Wide Field-of-view Sensor (SeaWiFS), Multispectral Thermal Imager (MTI), Adavanced Land Imager (ALI), and Hyperion instruments from the ROLO model.

Contact: Jim Butler, James.J.Butler@nasa.gov

Diffuser Calibration Facility (DCaF)

The Diffuser Calibration Facility (DCaF) has operated within Code 920 since May 1993. The facility is a class 10,000 cleanroom containing a unique, state-of-the-art, out-of-plane optical scatterometer. This scatterometer is capable of measuring the bi-directional scatter distribution function (BSDF is a term which includes bi-directional reflective and transmissive distribution function measurements (i.e. BRDF and BTDF)) of transmissive or reflective, specular or diffuse optical elements and surfaces in addition to granular, powdered, or liquid samples. The facility is considered a secondary standards calibration facility with measurements directly traceable to the Spectral Trifunction Automated Reflection Radiometer (STARR) located at the National Institute of Standards and Technology (NIST) in Gaithersburg, Maryland. BSDF measurements are made at any incident and scatter angle above or below a sample. The scatterometer employs incoherent and coherent monochromatic light sources. The incoherent source is a xenon arc lamp and 0.25 m Czerny-Turner monochromator. The current operating wavelength range of this source is 230 to 900 nm with an adjustable bandwidth between 4 and 10 nm. The coherent sources include He/Ne lasers at 543.5, 594.1, 612.0, and 632.8 nm and a He/Cd laser at 325.4 nm. The scatterometer is capable of polarized or unpolarized measurements using all sources. The sample stage can support samples up to 12 inches on a side and weight up to 10 lbs. Samples can also be rastered for reflectance or tranmittance uniformity. Scatterometer receivers include uv-sensitive and visible silicon photodiodes and photomultiplier tubes. The data acquisition electronics include programmable preamps matched to each detector and a programmable dual channel lock-in amplifier. The scatterometer is completely automated and data is displayed in real time. In year 2002, the facility commissioned an 8 degree directional/hemispherical reflectance measurement capability for diffuse reflective samples. This measurement complements and validates the alternative approach of integrating BRDF over the complete scattering hemisphere of a sample to determine hemispherical scatter.

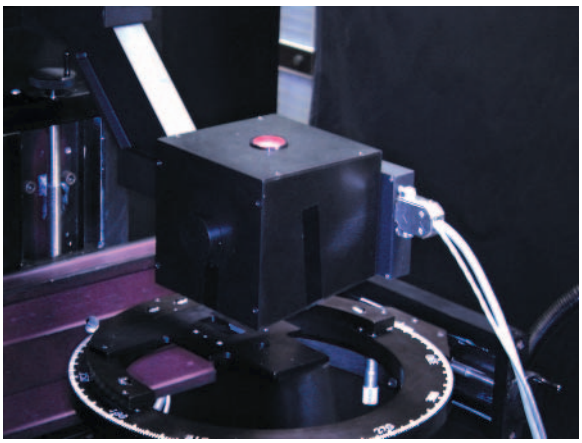

The measurement uncertainty of DCaF BSDF measurements is 0.7% (k=1), and agreement between absolute BSDF measurements made by the DCaF and by NIST on identical samples is 1% or better over the complete wavelength and angular operating ranges of the scatterometer. The measurement uncertainty of DCaF 8 degree directional/hemispherical measurements is 0.2% (k=1) over the complete operating wavelength range.

Figure 34. Integrating sphere/detector attachment to the scatterometer permits the direct measurement of 8 degree directional hemispherical scatter from optical surfaces.

In calendar year 2002, the facility installed an imaging microscope for sample inspection, and commissioned a materials solar exposure capability designed to mimic the on-orbit degradation of optical surfaces.

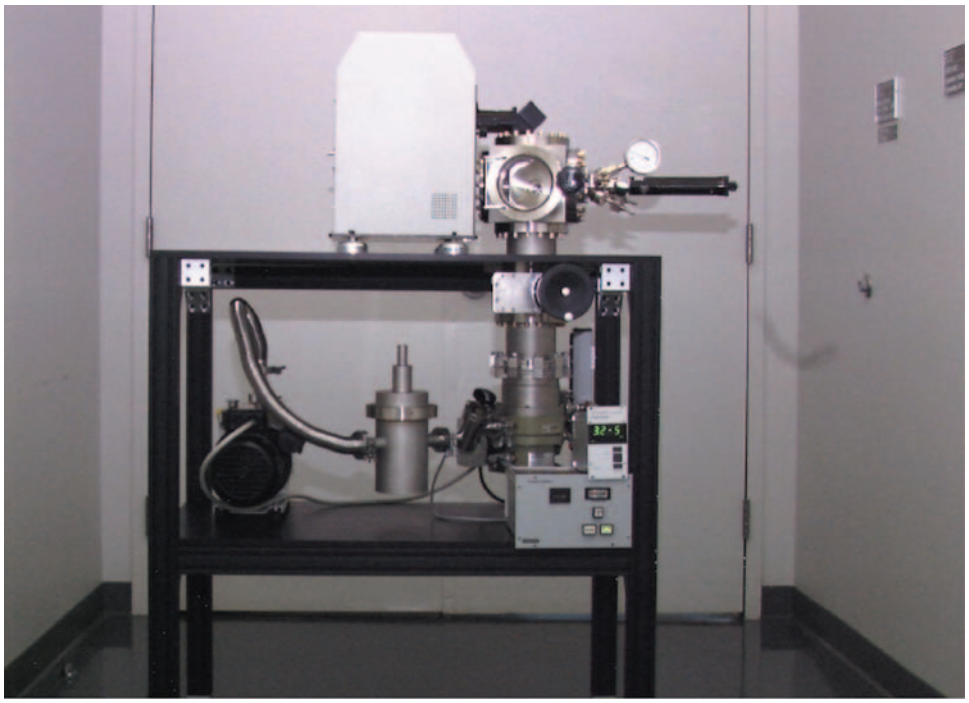

Figure 35. The Diffuser Calibration Facilities materials testing capability enables the controlled exposure of optical components to solar and contamination environments experienced on-orbit. Pre- to post-exposure changes in the optical properties of the components are measured on the facility scatterometer.

Since 1993, the DCaF has literally made tens of thousands of scatter measurements for flight and non-flight projects from both the government and private sectors. In calendar year 2002, the

DCaF provided scatter measurements to the following flight and non-flight projects in accordance with established flight and deployment schedules.

NASA SIMBIOS Calibrations:

In April and June of 2002, NASA's Sensor Intercomparison and Merger for Biological and Interdisciplinary Oceanic Studies (SIMBIOS) project became a new customer of the DCaF. In support of this project, the DCaF made BRDF measurements of three Spectralon diffusers used in the calibration of ocean color validation instruments. These measurements were made at 5 wavelengths between 400 and 900nm, at normal incidence, and over scatter angles of 42 to 48 degrees. One of the three samples was raster scanned to determine its BRDF uniformity.

Stereo COR-1 and COR-2 Calibrations:

The COR-1 project in the Solar Physics Branch was a repeat customer of the DCaF in 2002. The DCaF successfully measured the BTDF of 10 opal glass samples at normal illumination using a He/Ne laser at 632.8 nm and over a range of in- and out-of-plane scatter angles. The COR-1 project used these DCaF results in the evaluation of candidate opal glass diffusers for on-orbit flat-fielding of the COR-1 detector array. In addition to the opal glass samples, the DCaF used the He/Ne laser source to measure the BTDF of two neutral density filters for the COR-1 project.

The related COR-2 project was a new DCaF customer in 2002. The DCaF measured specular scatter from a highly polished aluminum mirror and glass sample. These measurements were made using the facility He/Ne laser at 632.8 nm and the monochromator-based source at 632.8 nm and 700 nm. The samples were illuminated normally and scatter was measured over a ±80 degree angular range. These results were used in evaluating the ability of aluminum mirrors and glass to act as heat rejection optics in the COR-2 instrument.

NASA Stennis Tarp Calibrations:

The DCaF made an extensive series of BSDF measurements for NASA's Stennis Commerical Remote Sensing Program Office on 4 tarp samples used in the vicarious calibration of commercial satellite sensors. The samples were measured at 485, 550, 633 (i.e. laser and monochromatic sources), and 800 nm over a large range of incident and scatter elevation and azimuthal angles. The effect of tarp weave orientation with respect to incident illumination and reflected scatter was quantified. The 8 degree directional hemispherical reflectance of the tarps was also measured at the aforementioned 4 wavelengths.

Mars Regolith Simulant BRDF Measurements:

In an effort to illustrate the versatility of the DCaF scatterometer, a granular sample of Mars Regolith Simulant from Johnson Space Center (JSC). The JSC MARS-1 sample is the < 1 mm diameter fraction of weathered volcanic ash from Pu'u Nene, a cinder cone on the island of Hawaii, which has been repeatedly cited as a close spectral analog to the bright Mars regions. This sample was measured from 250 to 900 nm over a range of incident and scatter angles from 0 to ±60 degrees. The sample reflectance was measured up to ±10 degrees out-of-plane and its 8 degree directional/hemispherical reflectance was quantified over the 250 to 900 nm wavlength range.

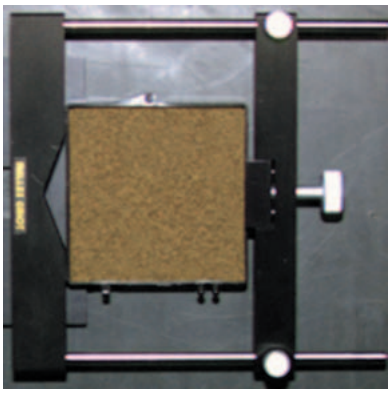

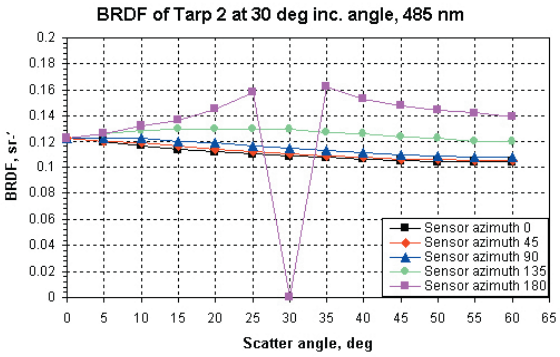

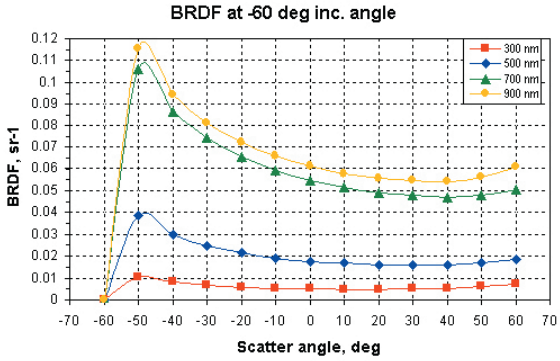

Figure 3. NASA's Stennis tarp (left) and NASA's JSC Mars simulated regolith sample 1 (right) images and BRDF results. The optical scatter from these un-conventional, different sample types is easily measured by the DCaF scatterometer.

Future Work:

In 2003, a scatterometer measurement capability from 1.0 micron to 2.5 microns using laser and monochromatic sources will be commissioned. In addition, work on improving the near-specular measurement of mirrors, designing and implementing an innovative, high precision, non-invasive sample alignment method, and designing and adding a controlled contaminant introduction system to the materials exposure capability will continue.

Contact: Jim Butler, James.J.Butler@nasa.gov

Calibration Facility

Figure 39, a photograph of "Hardy" together with its power supply and data collection console, is the largest (1.8 m diameter) and most intense of our sources. A ring of tungsten halogen lamps inside the source, behind the wire harness visible in Figure 34, is driven by a set of DC power supplies, with the current stabilized to better than ± 0.01%. This level of stabilization is necessary to reduce the corresponding changes in spectral radiance at the most sensitive wavelength (400 nm) to less than ± 0.1%. Barium sulfate paint, containing a small amount of polyvinyl alcohol as a binder, coats the interior surfaces of the source. This material is highly reflecting at wavelengths below 1μm, resulting in a large number of diffuse reflections for those photons emitted from the lamp filaments that successfully exit through the source aperture. Consequently, spectral radiance uniformity across the 25 cm diameter exit aperture is better than ± 0.2% for wave-

lengths below 1 μm, and is almost as uniform at higher wavelengths.

Sources are calibrated approximately every month relative to a NIST standard irradiance lamp. This procedure is necessary to offset slow degradation in radiance output caused by aging of the lamps within the source and the barium sulfate paint (usually a few percent per annum). With the wealth of supporting information collected on temperature, humidity, lamp voltages and lamp usage times, etc., we hope to build a predictive ability for identifying lamps and other components in the early stages of failure and to forecast changes in spectral radiance.

The Calibration Facility maintains several sources, each intended for a particular range of activities. Our 1.2 m diameter hemisphere source ("Laurel") is particularly useful when large diameter exit apertures are required, or when laboratory space is limited. Laurel has been used, for example, to assess the uniformity of response of the EPIC camera system on the Triana spacecraft. This work, completed in 2000, required an unusually large source diameter of over 45 cm. Another popular source, identified as "Slick", uses internal plates of polytetrafluoroethylene (PTFE) to scatter light emitted by the lamp filaments. PTFE is preferable to barium sulfate in that it contains negligible amounts of water and it has a higher reflectivity beyond a wavelength of 1μm. Occasionally the sources themselves travel to sites around the world. In recent years Calibration Facility staff and equipment have advanced NASA field programs in Portugal, Brazil, Japan and Canada, as well as many American states.

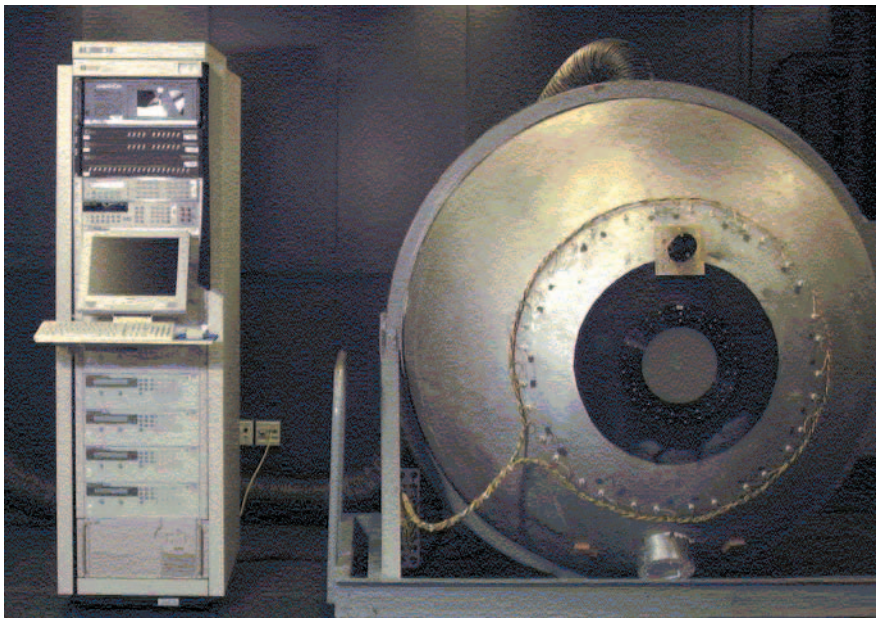

Figure 39. "Hardy", a calibration source.

The Calibration Facility usually houses its radiance sources in class M 5.5 clean rooms, implying that the density of airborne particles with a diameter of 0.5μm or greater is less than $10^{5.5}$, or 353,000 per cubic meter. The clean room air within the sources is further controlled in temperature and humidity.

The Calibration Facility's primary source calibration instrument is an Optronic Laboratory model 746 monochromator with an integrating sphere irradiance collector (746/ISIC). The 746/ISIC is calibrated in irradiance response prior to each measurement using a 1000 W quartz-halogen standard irradiance lamp that is traceable to NIST irradiance standards, and in wavelength using conventional line source lamps and lasers. Using silicon photodiode and lead sulfide detectors, the 746/ISIC transfers the irradiance calibration from the standard lamp to the sphere source being

measured. Knowledge of the aperture areas of the sphere under test and the ISIC collection sphere coupled with a measurement of the distance between the two apertures enables the radiance of the sphere source to be calculated. In the visible/near infrared wavelength region from 400 nm to 1000 nm, the 746/ISIC obtains data in 10 nm steps with a bandwidth of 10 nm. In the short-wave infrared wavelength region from 1000 nm to 1600 nm, data is obtained every 20 nm with a bandwidth of 20 nm. In the wavelength region from 1600 nm to 2500 nm, data is obtained every 20 nm with a bandwidth of 40 nm.

Although the primary customers of the Calibration Facility directly support the EOS Project, anyone interested in using the Calibration Facility is encouraged to contact our group. Provided the proposed work advances NASA's interests, we will be delighted to provide calibration services on a time-available basis and negotiable cost. Our website address is www.spectral.gsfc.nasa.gov, which we share with the Diffuser Calibration Facility. Further details, including source spectral radiance uncertainty estimates, were contained in the annual report for 2001.

Achievements in 2002:

The Environmental Control System (ECS) was installed and successfully tested in March 2002. The ECS dries and cools the air within "Hardy", shortening the warm-up time of the source and increasing the stability of spectral radiance within water vapor bands. The Temperature and Humidity Monitoring System (THMS) was also completed in March. Temperature and humidity data from critical points within the source system are now routinely recorded into the data system whenever the lamps inside the source are illuminated.

A paper describing monitoring and stability results was presented at SPIE's 9th International Symposium on Remote Sensing, Crete, Greece.

In May 2002 the electronics and software for the rebuilt Calibration Transfer System (CTS 750) was completed, and work began on characterizing it and comparing its performance with the operational system (known as the CTS 746 system).

Code 900 used the Calibration Facility during the year to calibrate a large number of Cimel sun photometers returned to GSFC for calibration from AERONET sites around the world. GSFC radiometers such as the Cloud Absorption Radiometer (CAR), Sensor Integration and Modeling for Biological Agent Detection (SIMBAD) radiometers from the SIMBIOS program, and several spectrometer systems and sources associated with the Landsat and MODIS projects were either calibrated or had their calibration compared with independent standards during the year, and calibration work associated with the second SIMBIOS Radiometric Intercomparison (SIMRIC-2) was performed.

The MErcury Surface, Space ENvironment, GEochemistry and Ranging mission (MESSENGER) includes the Mercury Laser Altimeter (MLA). MLA's out-of-field stray light was measured in the Calibration Facility in September, and found to be within 20% of the theoretical worst-case value.

Spectrometers from NASA's Langley Research Center and the University of Maryland were calibrated during the year, and several sources were calibrated at NASA's Ames Research Center (ARC) at the request of ARC. NASA's Wallops Flight Facility requested and received calibration support for one of their sources.

Contact: Peter Abel, Peter.Abel-1@nasa.gov

Refereed Journal Publications:

Degnan, J.J., "A conceptual design for a spaceborne 3D imaging lidar", J. e&i Elektrotechnik und Informationstechnik, Vol. 4, pp. 99-106, 2002.

Degnan, J.J., "Photon-counting multikilohertz microlaser altimeters for airborne and spaceborne topographic measurements", J. Geodynamics, Special Issue on Laser Altimetry, Vol. 34, pp.503-549, 2002.

Degnan, J.J., "Asynchronous laser transponders for precise interplanetary ranging and time transfer", J. Geodynamics, Special Issue on Laser Altimetry, Vol. 34, pp. 551-594, 2002.

Drake, J. B., R. Dubayah, D. B. Clark, R. G. Knox, **J. B. Blair**, M. A. Hofton, R. L. Chazdon, R. L. Weishampel, and S. Prince, Estimation of tropical forest structural characteristics using large-footprint lidar, Remote Sensing of Environment, 79: 305-319, 2002.

Drake, J. B., R. Dubayah, R. Knox, D. B. Clark, and **J. B. Blair**, Sensitivity of large-footprint lidar to canopy structure and biomass in a neotropical rainforest, Remote Sensing of Environment, 81:378-392, 2002.

Hofton, M. A. and **J. B. Blair**, Laser altimeter return pulse correlation: A method for detecting surface topographic change, Journal of Geodynamics, 34:477-489, 2002.

Hofton, M. A., **L. E. Rocchio, J. B. Blair** and R. Dubayah, Validation of vegetation canopy lidar sub-canopy topography measurements, Journal of Geodynamics, 34:491-502, 2002.

Mallama A.J. and **J.J. Degnan**, "A thermal infrared cloud mapper for observatories", Publications of the Astronomical Society of the Pacific", Vol. 114, pp.913-917, 2002

Zwally, H.J., B. Schutz, W. Abdalati, **J. Abshire**, C. Bentley, A. Brenner, **J. Bufton**, J. Dezio, D. Hancock, **D. Harding**, T. Herring, B. Minster, K. Quinn, S. Palm, J. Spinhirne, R. Thomas, " ICESat's laser mreasurements of polar ice, atmosphere, ocean and land," Journal of Geodynamics, Vol 34, 405-445, 2002.

Proceedings Papers, NASA Technical Reports, etc.

Abshire, J.B., X. Sun, **E.A. Ketchum, P.S. Millar, H. Riris**, "Geoscience Laser Altimeter System (GLAS) for the ICESat Mission, " IEEE IGARSS-02 conference, paper xx, Toronto Canada, June 24-28, 2002.

Andrews, A. E., "CO_2 Measurements from Space: Possibilities and Possible Pitfalls," Carbon Data Assimilation Workshop, National Center for Atmospheric Research, Boulder, CO 20-31 May 2002.

Andrews, A. E., J. F. Burris, **J. B. Abshire**, M. A. Krainak, **H. Riris, X. Sun**, **G. J. Collatz**, "A Ground-Based Profiling Differential Absorption LIDAR System for Measuring CO2 in the Planetary Boundary Layer" Carbon Cycle Science: The North American Carbon Program" special session of the Fall 2002 Meeting of the American Geophysical Union, San Francisco, California, 6-10 December 2002.

Butler, J.J., P.Y. Barnes, E.A. Early, C. van Eijk-Olij, A.E. Zoutman, S. van Buller-Leeuwen, and J.G. Schaarsberg, "Comparison of Ultraviolet Bidirectional Reflectance Distribution Function (BRDF) Measurements of Diffusers Used in the Calibration of the Total Ozone Mapping Spectrometer (TOMS)", Proceedings of the 9th International Symposium on Remote Sensing, Agia Pelagia, Crete, 2002..

Carter, D., "System Upgrades of the NASA SLR Network", Proceedings of the 13th International Workshop on Laser Ranging, October 7-11,2002, Washington, D.C.

Georgiev, G. and **J.J. Butler**, "Bidirectional Reflectance Distribution Function and Hemispherical Reflectance of JSC Mars-1," SPIE Proceedings on Surface Scattering and Diffraction for Advanced Metrology II, Seattle, Washington, 2002.

Degnan, J.J., "SLR2000: Progress and Future Applications", Proceedings of the 13th International Workshop on Laser Ranging, October 7-11,2002, Washington, D.C.

Degnan, J.J.,"Optimization of the Correlation Range Receiver Parameters in SLR2000", Proceedings of the 13th International Workshop on Laser Ranging, October 7-11,2002, Washington, D.C.

Mallama, A., **J. J. Degnan**, F. E.Cross, J. M. Mackenzie, "Infrared Sky Camera -- The Production Mode", Proceedings of the 13th International Workshop on Laser Ranging, October 7-11,2002, Washington, D.C.

McGarry, J., T. Zagwodzki, J.J. Degnan, "SLR2000 Closed Loop Tracking with a Photon-Counting Quadrant Detector", Proceedings of the 13th International Workshop on Laser Ranging, October 7-11, 2002, Washington, D.C.

McGarry, J., J. Cheek, A. Mallama, R. Ricklefs, A. Mann, M. Perry, J. Horvath, R. Barski, "SLR2000 Software: Current Test Results and Recent Developments", Proceedings of the 13th International Workshop on Laser Ranging, October 7- 11, 2002, Washington, D.C.

Meister G, **P. Abel**, R. Barnes, J. Cooper, C. Davis, M. Godin, D. Goebel, G. Fargion, R. Frouin, D. Korwan, R. Maffione, C.McClain, S.McLean, D. Menzies, A. Poteau, J.Robertson, J. Sherman, "The first SIMBIOS Radiometric Intercomparison (SIMRIC-1), April - September 2001", NASA/TM-2002-210006, March 2002.

Marketon J., **Peter Abel, James J. Butler**, Gilbert R. Smith, John W. Cooper, "Integrating sphere source monitoring and stability data", SPIE 9th International Symposium on Remote Sensing, Crete, Greece, 2002.

Patterson, D., **J. McGarry**, "Overview of Data for the SLR2000 Tracking Mount", Proceedings of the 13th International Workshop on Laser Ranging, October 7-11,2002, Washington, D.C.

Sun, X. and **J.B. Abshire**, "Performance of a breadboard lidar receiver at 1570nm for remotely sensing atmospheric CO2 concentrations," *Conference on Laser and Electro-Optics (CLEO),* May 20-24, 2002, Long Beach, CA, Paper CFF3.